International Journal of Solids and Structures 48 (2011) 3129–3141

Contents lists available at ScienceDirect

International Journal of Solids and Structures

journal homepage: www.elsevier.com/locate/ijsolstr

A theoretical treatment on the mechanics of interfaces in deformable porous media

Franck J. Vernerey

Department of Civil, Environmental and Architectural Engineering, University of Colorado, Boulder, CO, USA

ARTICLE INFO

Article history:
Received 3 March 2011
Received in revised form 29 April 2011
Available online 21 July 2011

Keywords:
Interface mechanics
Porous media

ABSTRACT

The presence of interfaces (such as cracks, membranes and bi-material boundaries) in hydrated porous media may have a significant effect on the nature of their deformation and interstitial fluid flow. In this context, the present paper introduces a mathematical framework to describe the mechanical behavior of interfaces in an elastic porous media filled with an inviscid fluid. While bulk deformation and flow are characterized by displacement gradient and variations in the fluid chemical potential, their counterpart in the interface are derived by defining adequate projections of strains and flow onto the plane of the interface. This operation results in the definition of three interface deformation and stress measures describing decohesion, mean tangential strain and relative tangential strain, as well as three interface fluid driving forces and flux representing normal flux, mean tangential flux and relative tangential flux. Consistent with this macroscopic description of interface behavior, a set of governing equations are then introduced by considering the conservation of mass and the balance of momentum in the mixture. In particular, we show that the coupled mechanisms of interface deformation and fluid flow are described by six differential equations for fluid flow and three equations for solid deformation. It is also shown that a simpler set of governing equation can be derived when incompressible constituents are considered. The behavior of the mixture is finally specified through a general linear constitutive relation that relies on the definition of quadratic strain energy and dissipation functions. While an large number of material constants are needed in the general case, we show that under simplifying assumptions, the behavior of the interface can be written in terms of only eight material constants. A summary and discussion is then provided on the proposed formulation and potential applications are suggested.

1. Introduction

Studies on the mechanics of hydrated porous media (composed of a deformable solid skeleton and an interstitial fluid phase) are of great interest to understand the behavior of a variety of materials such as biological tissues, soils or hydrogels. The theory of porous media, originally introduced by Biot (1941, 1957) in the context of consolidation and later generalized to the theory of mixtures, notably by Bowen (1980), Truesdell (1969) and Rajagopal and Tao (1995) has been very successful at describing the combined fluid flow and solid deformation in porous media. These continuum theories are based on the hypothesis that porous media are composed of a macroscopically homogeneous interconnected porous network and therefore can be macroscopically described in terms of continuous fields (such as solid displacement and fluid velocities). However, the microstructure of porous materials is sometimes characterized by the presence of interfaces, such as cracks, membranes and thin material interfaces, introducing strong and weak discontinuities in displacement fields. These discontinuities may critically affect the mechanical behavior of the medium and the nature of the interstitial fluid flow within the solid. In this context, the presence of cracks on interstitial fluid flow has been the object of various studies (Barthelemy, 2009; Liolios and Exadaktylos, 2008; Pouya and Ghabezloo, 2008; Ghabezloo and Pouya, 2008), particularly in the situation where the solid phase does not deform. For instance, one strategy consists of modeling interfaces (cracks) as thin ellipsoidal inclusions for which an effective permeability can be derived using self-consistent homogenization techniques (Dormieux and Kondo, 2007; Barthelemy, 2009). An alternative approach was presented by Liolios and Exadaktylos (2008) in which fluid flow in non-intersecting cracks was described in terms of a line of discontinuity. This formulation was more recently extended by Pouya and Ghabezloo (2008) to describe intersecting cracks, which further allowed to estimate the effective permeability of a micro-cracked porous medium. While the above studies provide very good estimations of fluid flows within cracks (and can be extended to arbitrary porous interfaces), they did not consider the effect of solid deformation, as applications mainly focused on rigid media such as rock and concrete.

With different applications in mind, the mechanical deformation of interfaces in elastic solids was explored by Gurtin et al. (1998) within the context of small deformations. Viewing interfaces as lines of discontinuity in displacement and strain fields, various measures

E-mail address: franck.vernerey@colorado.edu

0020-7683/$ - see front matter © 2011 Elsevier Ltd. All rights reserved.
doi:10.1016/j.ijsolstr.2011.07.005

of interface stress and deformation could be introduced including decohesion, interface tangential strain and relative strain. This formulation lately provided a strong basis onto which the effect of surface stresses in nano-materials (Yvonnet et al., 2008; Farsad et al., 2010) and the elasticity of biological cell membrane (Vernerey and Farsad, 2011) could be incorporated within the context of continuum mechanics. There are, however, many situations where interstitial fluid flow and solid deformation are not independent. These situations occur either when solid deformations are significant enough to trigger a change in interface porosity and aperture or when fluid pressure is large enough to create interface deformation. The first case typically occurs in soft hydrated materials, such as hydrogels and biological tissues in which the deformation of membranes or cracks generate fluid motion. The second case typically occurs in geomechanical fracture systems, in which high fluid pressure induce crack opening (McDermott and Kolditz, 2006). Existing research has mainly concentrated on the case of cracks in deformable media. For example, Rethore et al. (2007, 2008) introduced a two-scale numerical formulation that couple the balance equation of a poro-elastic medium (macro-scale) with the equations describing the flow of a viscous fluid through a cavity (micro-scale). This approach could naturally be implemented within an enriched finite element framework to explore the combined deformation/flow properties of fractured media. A similar framework was also employed by Zhou et al. (2008) to model the flow of water through a deformable solid containing a network of interconnected cracks. However, while studies on fracture media is critical, there are many situations in which interfaces possess their own properties (porosity, elasticity); this is, for instance, the case of biological membranes between two porous solids. In such cases, the deformation of the membrane is not only characterized by the relative displacement between the two sides (such as for cracks), but it is also represented by tangential strain (associated with surface tension). Similarly, fluid flow is not necessarily tangential to the interface, but according to the interface permeability, a normal flow may exist across the interface.

To address these issues and generalize current formulations to a larger variety of material's interfaces, this paper explores a unified continuum framework, originally based on the approach of Gurtin et al. for single phase solids (Gurtin et al., 1998). Considering interfaces whose thickness is significantly smaller than the typical length-scale of applications (size of solid, characteristic length scale of physical processes), interfaces are modeled as two-dimensional surfaces Γ across which continuum fields (such as displacement, strain, fluid pressure and pressure gradient) are discontinuous. The nature of the discontinuities enables us to define a variety of deformation measures and fluid driving forces associated with the interface. In particular, a set of three deformation and fluid driving forces are introduced, leading to an equal number of stresses and flow in the interfaces: a cohesive stress, resisting the separation of two sides of the interface, a surface stress, characterizing the tangential tension and a surface couple stress, which resist heterogeneous deformation across the interface. In analogy, interface fluid flow is described with (a) a normal flux crossing the interface, (b) a tangential flux and (c) a differential tangential flux along Γ. Using a two-scale view of the interface (microscale-macroscale) and using thickness averaging techniques and variational principles, a set of governing equations is derived in order to satisfy both mass conservation and momentum balance. In the general case, the derived equations are able to describe the coupled deformation-flow mechanisms occurring in the interface and their interactions with the bulk. We give particular attention to the case in which constituents are incompressible, a common assumption for most biological materials. The formulation is then completed by introducing linear constitutive equations that relate strain and fluid driving force to stress measures and fluid flux.

The general organization of the paper is as follows. In the next section, we define few notations and mathematical concepts that are useful for the remainder of the paper. Section 3 then introduces kinematics quantities and thermodynamic forces that lead to clear definitions of solid and fluid motion in porous media with interfaces. This section also establishes a relationship between macroscopic and microscopic description of interfaces. Sections 4 and 5 then focus on the derivation of coupled equations of mass and momentum balance that govern the solid deformation and fluid flow in the bulk and interfaces. A set of linear constitutive relations is then provided in Section 6, followed by a short discussion and conclusion in Section 7.

2. Mathematical and physical preliminaries

2.1. Interface thickness averaging

Let us consider a porous solid, contained in a closed domain Ω, delimited by a boundary $\partial\Omega$ in a three-dimensional space associated with a cartesian coordinate system x_i, $\{i = 1,2,3\}$. In addition to an interconnected network of pores, the interior of this solid is characterized by the existence of interfaces (denoted by Γ) whose geometry is characterized by the fact that their thickness is negligible compared to the others dimensions. As a consequence, two different views may be adopted in their analysis: a microscale and a macroscale description. At the "microscale", interfaces can be represented by thin layers of finite thickness h, associated with a local coordinate system (ξ_n, ξ_s, ξ_t) whose unit vectors points along the normal and tangential directions of Γ (Fig. 1). At the "macroscale", interfaces are described as zero-thickness surfaces whose orientation is described by a unit vector field $\mathbf{n}$, indicating the normal direction to the plane tangent to Γ at this point (Fig. 1). In this work, we assume that interfaces Γ may intersect with the boundary $\partial\ \Omega$ but do not intersect with one another. In other words, interface boundaries, defined by a curve ℓ, can be decomposed into an external boundary ℓ_e such that $\ell_e = \partial\Omega \cap \Gamma$ and an internal boundary ℓ_i such that $\ell = \ell_i \cup \ell_e$. To reconcile the macroscopic and microscopic description of the interface, a thickness averaging operation is defined such that a microscopic field $\tilde{\mathbf{a}}$ is related to macroscopic mean fields $\langle\tilde{\mathbf{a}}\rangle$ and $\langle\langle\tilde{\mathbf{a}}\rangle\rangle$ as:

$$\langle\tilde{\mathbf{a}}\rangle = \frac{1}{h}\int_{-h/2}^{h/2} \tilde{\mathbf{a}}\, d\xi_n \quad \text{and} \quad \langle\langle\tilde{\mathbf{a}}\rangle\rangle = \frac{1}{h}\int_{-h/2}^{h/2} \frac{\partial\tilde{\mathbf{a}}}{\partial\xi_n}\, d\xi_n. \tag{1}$$

In the above definitions, the operation $\langle\cdot\rangle$ defines the average of $\tilde{\mathbf{a}}$ across the interface while the quantity $\langle\langle\cdot\rangle\rangle$ is a measure of the mean variation of $\tilde{\mathbf{a}}$ along the normal direction $\mathbf{n}$. These expressions will be useful to maintain a detailed macroscopic description of the interface in terms of porosity, flux and deformation as seen in the reminder of this paper. At this point, it is important to introduce a continuum description of the material porosity in the bulk (denoted as ϕ) and in the interface, in which we introduce macroscopic porosities $\bar{\phi}$ and $\bar{\bar{\phi}}$ of the form:

$$\bar{\phi} = \langle\tilde{\phi}\rangle \quad \text{and} \quad \bar{\bar{\phi}} = \langle\langle\tilde{\phi}\rangle\rangle, \tag{2}$$

where $\tilde{\phi}$ is the microscale interface porosity, whose value may differ from that of the bulk. The above macroscopic quantities represent the average porosity and the average normal variation of porosity within the interface. In addition, for saturated mixtures, the volume fraction $\tilde{\phi}^f$ of fluid is such that $\tilde{\phi}^f = \tilde{\phi}$; this implies that macroscopic volume fraction of fluid and solid are described by the quantities:

$$\bar{\phi}^f = \bar{\phi}, \quad \bar{\bar{\phi}}^f = \bar{\bar{\phi}}, \quad \bar{\bar{\phi}}^s = -\bar{\bar{\phi}} \tag{3}$$

where the macroscopic volume fractions $\bar{\phi}^f, ;\bar{\bar{\phi}}^f, \bar{\phi}^s, \bar{\bar{\phi}}^s$ of fluid and solid are calculated from the microscopic fractions $\tilde{\phi}^f$ and $\tilde{\phi}^s$ through average relation as given in (2).

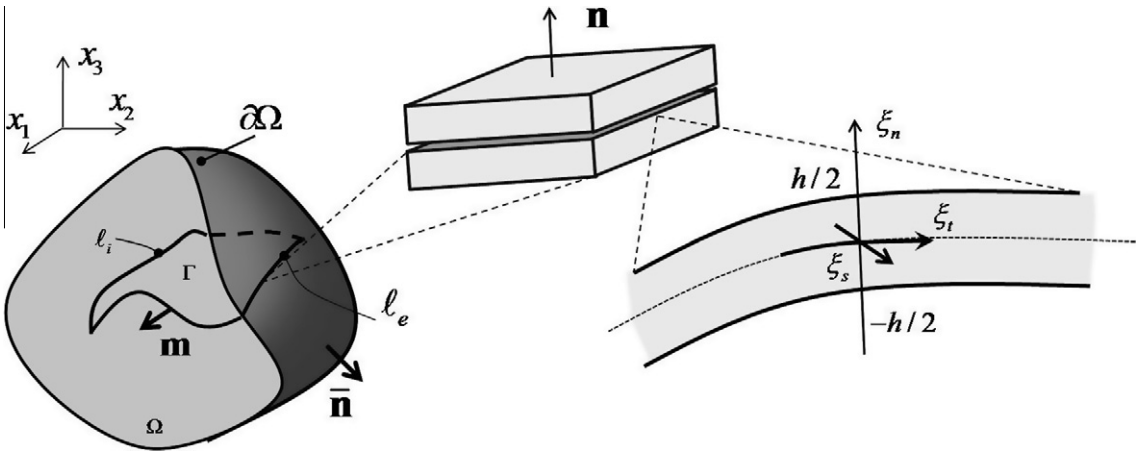

Fig. 1. Porous solid Ω containing interfaces Γ and the normal vector to interfaces.

2.2. Surface operations and projections

Before we define the kinematics of deformation and flow within interfaces, it is important to discuss some useful mathematical concepts related to the projection of vector and tensor fields on two-dimensional surfaces. Let us first consider a surface Γ in a three-dimensional domain Ω across which a continuum field $\mathbf{a}$ (that can be a scalar, a vector or a tensor) is discontinuous. Let us denote as $\mathbf{a}^+$ and $\mathbf{a}^-$ the value of this field on each side of Γ. The jump, or discontinuity, of $\mathbf{a}$ across Γ is denoted by:

$$[\mathbf{a}] = \mathbf{a}^+ - \mathbf{a}^- \tag{4}$$

while the mean of $\mathbf{a}$ across Γ is represented by:

$$\{\mathbf{a}\} = \frac{1}{2}(\mathbf{a}^+ + \mathbf{a}^-) \tag{5}$$

To carry out our analysis of interface description, let us consider an arbitrary vector field $\mathbf{a}(\mathbf{x})$ and a second order tensorial field $\mathbf{T}(\mathbf{x})$, both continuous and differentiable fields in $\Omega - \{\Gamma\}$. It is now of interest to project such continuous fields onto an interface Γ through the following normal and tangential projection operators:

$$\mathbf{P}^{\perp} = \mathbf{n} \otimes \mathbf{n} \quad \text{and} \quad \mathbf{P}^{\parallel} = \mathbf{I} - \mathbf{n} \otimes \mathbf{n}, \tag{6}$$

respectively, where $\mathbf{n}$ is the unit vector that is normal to Γ. In the above equation, $\mathbf{I}$ is used for the second rank identity tensor in three dimensions and the symbol $\otimes$ is used for the vector direct product. This operator enables us to decompose vector field $\mathbf{a}$, into normal and tangential contributions ($\mathbf{a}^{\perp}$ and $\mathbf{a}^{\parallel}$, respectively) along the interface as follows (Fig. 2):

$$\mathbf{a} = \mathbf{a}^{\perp} + \mathbf{a}^{\parallel} \quad \text{where } \mathbf{a}^{\perp} = \mathbf{P}^{\perp} \cdot \mathbf{a} \quad \text{and} \quad \mathbf{a}^{\parallel} = \mathbf{P}^{\parallel} \cdot \mathbf{a}. \tag{7}$$

A similar decomposition can be achieved for the gradient $\nabla\mathbf{a}$ in the form:

$$\nabla\mathbf{a} = (\nabla\mathbf{a})^{\perp} + (\nabla\mathbf{a})^{\parallel} \quad \text{where } (\nabla\mathbf{a})^{\perp} = \nabla\mathbf{a} \cdot \mathbf{P}^{\perp} \quad \text{and} \quad (\nabla\mathbf{a})^{\parallel} = \nabla\mathbf{a} \cdot \mathbf{P}^{\parallel}. \tag{8}$$

In the above expression, it is understood that $(\nabla\mathbf{a})^{\perp}$ and $(\nabla\mathbf{a})^{\parallel}$ represent the gradient of $\mathbf{a}$ in a direction normal and tangential to the interface. The quantity $(\nabla\mathbf{a})^{\parallel}$ is therefore often denoted as the *surface gradient* of $\mathbf{a}$. Note that $\mathbf{a}$ and its gradient are not necessarily continuous across the interface Γ and the projection may lead to two different values according to the side of the interface considered. The decomposition of a tensor $\mathbf{T}$ may similarly be shown to take the form:

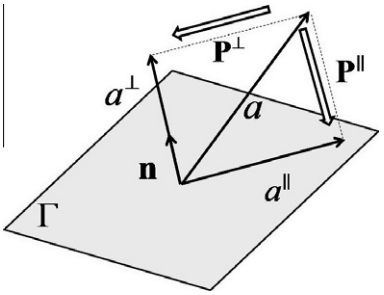

Fig. 2. Projection of a vector field onto an interface with normal unit vector $\mathbf{n}$.

$$\mathbf{T} = \mathbf{P}^{\parallel} \cdot \mathbf{T} \cdot \mathbf{P}^{\parallel} + \mathbf{P}^{\perp} \cdot \mathbf{T} \cdot \mathbf{P}^{\parallel} + \mathbf{P}^{\parallel} \cdot \mathbf{T} \cdot \mathbf{P}^{\perp} + \mathbf{P}^{\perp} \cdot \mathbf{T} \cdot \mathbf{P}^{\perp}, \tag{9}$$

where, we distinguish the parallel projection ($\mathbf{T}^{\parallel}$) and normal projection ($\mathbf{T}^{\perp}$):

$$\mathbf{T}^{\parallel} = \mathbf{P}^{\parallel} \cdot \mathbf{T} \cdot \mathbf{P}^{\parallel} \quad \text{and} \quad \mathbf{T}^{\perp} = \mathbf{P}^{\perp} \cdot \mathbf{T} \cdot \mathbf{P}^{\perp}. \tag{10}$$

which give a representation of the tensor $\mathbf{T}$ in the plane of the interface and in the direction normal to the interface, respectively. It is important to note that $\mathbf{T}^{\parallel}$ and $\mathbf{T}^{\perp}$ keep the same rank as $\mathbf{T}$; this feature is convenient when manipulating tensors and their projections within the same expressions. Finally, the divergence of $\mathbf{T}$ can similarly be decomposed into normal and tangential components as:

$$div\mathbf{T} = div^{\perp}\mathbf{T} + div^{\parallel}\mathbf{T} \quad \text{where } div^{\perp}\mathbf{T} = \nabla\mathbf{T} : \mathbf{P}^{\perp} \quad \text{and} \quad div^{\parallel}\mathbf{T} = \nabla\mathbf{T} : \mathbf{P}^{\parallel} \tag{11}$$

where we use the double tensor contraction ":" and $div^{\parallel}\mathbf{T}$ represents the surface divergence of a tensorial field. We note that once again, the projection of a tensor and its divergence may take different values according to the side of the interface considered.

3. Motion and forces in a biphasic medium with interfaces

3.1. Kinematics of deformation and stress fields

The kinematics of bulk and interface are now introduced from a macroscopic point of view. For this, the bulk domain is considered as a homogeneous medium in which solid motion is entirely defined by the knowledge of the displacement vector $\mathbf{u}(\mathbf{x})$, that is assumed to be continuous and differentiable everywhere in Ω, except on the interface Γ. Remaining in the context of small

deformations, the bulk strain and spin are represented by the symmetric tensor $\boldsymbol{E}$ and the antisymmetric tensor $\boldsymbol{W}$:

$$\boldsymbol{E} = \frac{1}{2}(\nabla\mathbf{u} + (\nabla\mathbf{u})^T) \quad \text{and} \quad \boldsymbol{W} = \frac{1}{2}(\nabla\mathbf{u} - (\nabla\mathbf{u})^T), \tag{12}$$

respectively, where ∇ is the differential operator and the superscript T denotes the transpose operator. In contrast to the bulk, interfaces are seen as lines of discontinuities in terms of displacement and strain fields. Based on this observation, various types of deformation can be associated with the interface as discussed by Gurtin et al. (1998). In this work, we describe interface deformation in terms of two modes that consist of (i) the mean interface displacement gradient $\boldsymbol{\Upsilon}_s$ in the interface and (ii) the relative interface displacement gradient $\boldsymbol{\Upsilon}_m$ across Γ. We next provide a definition of each deformation mode.

3.1.1. Mean interface displacement gradient

The mean displacement gradient tensor $\boldsymbol{\Upsilon}_s$ in Γ is defined as the mean displacement gradient on both side of Γ:

$$\boldsymbol{\Upsilon}_s = \{\nabla\mathbf{u}\} \tag{13}$$

where the definition of the notation $\{\cdot\}$ is given in (5). It can generally be decomposed into a tangential component $\boldsymbol{\Upsilon}_s^{\parallel}$ in the plane of the interface and a normal component, represented by the vector $\boldsymbol{\upsilon}_s^{\perp}$ such that:

$$\boldsymbol{\Upsilon}_s = \boldsymbol{\Upsilon}_s^{\parallel} + \boldsymbol{\upsilon}_s^{\perp} \otimes \mathbf{n}. \tag{14}$$

From this decomposition, two assumptions can be made regarding the deformation of the interface. First, to satisfy deformation compatibility between bulk and interface, the mean tangential displacement gradient is related to its bulk counterpart by:

$$\boldsymbol{\Upsilon}_s^{\parallel} = \mathbf{P}^{\parallel} \cdot \{\nabla\mathbf{u}\} \cdot \mathbf{P}^{\parallel} \tag{15}$$

where $\{\cdot\}$ represents the average of $\nabla\mathbf{u}$ on both sides of the interface. Similar to the displacement gradient in the bulk, $\boldsymbol{\Upsilon}_s^{\parallel}$ is comprised of a tangential strain component, denoted as $\boldsymbol{E}_s^{\parallel}$ and a tangential spin $\boldsymbol{W}_s^{\parallel}$, that induces rotation about the normal vector $\mathbf{n}$:

$$\boldsymbol{\Upsilon}_s^{\parallel} = \boldsymbol{E}_s^{\parallel} + \boldsymbol{W}_s^{\parallel} \quad \text{where} \begin{cases} \boldsymbol{E}_s^{\parallel} = \mathbf{P}^{\parallel} \cdot \{\boldsymbol{E}\} \cdot \mathbf{P}^{\parallel} \\ \boldsymbol{W}_s^{\parallel} = \mathbf{P}^{\parallel} \cdot \{\boldsymbol{W}\} \cdot \mathbf{P}^{\parallel}. \end{cases} \tag{16}$$

In addition, the normal component $\boldsymbol{\upsilon}_s^{\perp}$ of the interface average strain can be related to the relative displacement $[\mathbf{u}]$ between two sides of Γ as:

$$\boldsymbol{\upsilon}_s^{\perp} = [\mathbf{u}]/h \tag{17}$$

where the factor $1/h$ was incorporated for dimensional purposes. Because of the small value of h, the above definition implies that large normal strain can be obtained for relatively small values of displacement discontinuity $[\mathbf{u}]$. To circumvent this issue, the normal interface deformation is often characterized by the relative displacement $[\mathbf{u}]$ instead of $\boldsymbol{\upsilon}_s^{\perp}$. Such an approach is taken in the rest of this paper.

3.1.2. Relative interface displacement gradient

The jump in interface displacement gradient $\boldsymbol{\Upsilon}_m$ across the interface is measured by the discontinuity of displacement gradient projected onto Γ as follows:

$$\boldsymbol{\Upsilon}_m = \mathbf{P}^{\parallel} \cdot [\nabla\mathbf{u}]. \tag{18}$$

This tensor can generally be decomposed into a tangential component $\boldsymbol{\Upsilon}_m^{\parallel}$ and a normal component, represented by the vector $\boldsymbol{\upsilon}_m^{\perp}$ such that:

$$\boldsymbol{\Upsilon}_m = \boldsymbol{\Upsilon}_m^{\parallel} + \boldsymbol{\upsilon}_m^{\perp} \otimes \mathbf{n}. \tag{19}$$

The tangential projection $\boldsymbol{\Upsilon}_m^{\parallel}$ represents a combination of (a) a discontinuity $\boldsymbol{E}_m^{\parallel}$ in tangential strain and (b) a discontinuity $\boldsymbol{W}_m^{\parallel}$ in spin about the normal vector $\mathbf{n}$ such that:

$$\boldsymbol{\Upsilon}_m^{\parallel} = \boldsymbol{E}_m^{\parallel} + \boldsymbol{W}_m^{\parallel} \quad \text{where} \begin{cases} \boldsymbol{E}_m^{\parallel} = \mathbf{P}^{\parallel} \cdot [\boldsymbol{E}] \cdot \mathbf{P}^{\parallel} \\ \boldsymbol{W}_m^{\parallel} = \mathbf{P}^{\parallel} \cdot [\boldsymbol{W}] \cdot \mathbf{P}^{\parallel}. \end{cases} \tag{20}$$

Similarly, the discontinuous normal displacement gradient can be split into a component $\boldsymbol{e}_m^{\perp}$ arising from normal strain and a component $\boldsymbol{w}_m^{\perp}$ arising from a spin discontinuity about an axis that lies in the plane of the interface. We write:

$$\boldsymbol{\upsilon}_m^{\perp} = \boldsymbol{e}_m^{\perp} + \boldsymbol{w}_m^{\perp} \quad \text{where} \begin{cases} \boldsymbol{e}_m^{\perp} = \mathbf{P}^{\parallel} \cdot [\boldsymbol{E}] \cdot \mathbf{n} \\ \boldsymbol{w}_m^{\perp} = \mathbf{P}^{\parallel} \cdot [\boldsymbol{W}] \cdot \mathbf{n}. \end{cases} \tag{21}$$

A representation of the various interface strain measures is given in Fig. 3. To derive an objective theory, it is critical to ensure that the various measures of deformation are independent of rigid body rotation. Since $\boldsymbol{W}$ and $\boldsymbol{W}_s^{\parallel}$ are representative of rigid body rotation in the bulk and at the interface, they will not be considered as measures participating to interface deformation. However, one should note that $\boldsymbol{W}_m^{\parallel}$ and $\boldsymbol{w}_m^{\perp}$ are representative of spin discontinuities and may be thought as torsion-like deformation (Fig. 3). They therefore must be considered as relevant strain measures in the interface. As a result, interface deformation can be entirely described in terms of three strain measure $[\mathbf{u}], \boldsymbol{E}_s^{\parallel}$ and $\boldsymbol{\Upsilon}_m$, that denote the relative displacement on opposite sides of the interface, the mean tangential strain tensor and the relative interface displacement gradient, respectively. Note that these strain measures were introduced by Gurtin et al. (1998) in the context of a single solid constituent.

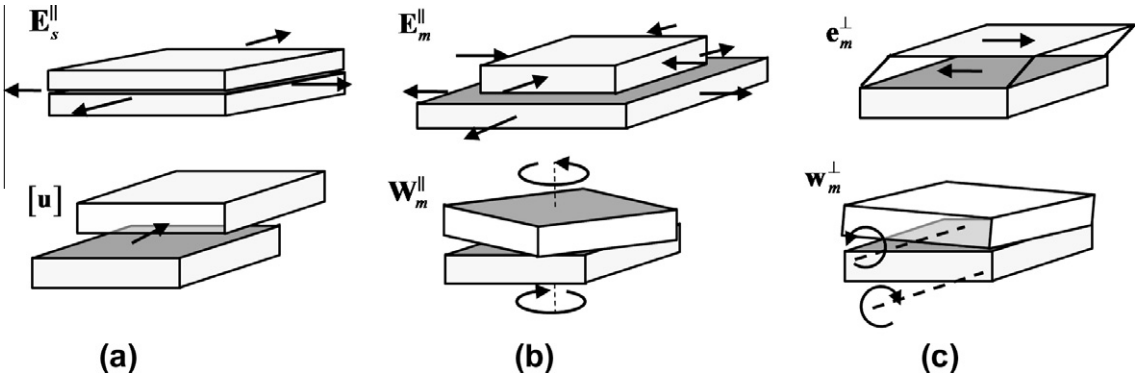

Fig. 3. Illustration of the interface strain measures. (a) Tangential and normal average strain. (b) Relative tangential strain and relative tangential spin. (c) Normal relative strain and normal relative spin.

3.1.3. Relationship between macroscopic and microscopic interface strains

To establish a relation between macroscopic and microscopic deformation, we first introduce the microscopic displacement gradient $\tilde{\boldsymbol{\chi}} = \partial\tilde{\mathbf{u}}/\partial\boldsymbol{\xi}$ where $\tilde{\mathbf{u}}(\xi_n, \xi_s, \xi_t)$ is the microscopic solid displacement that is measured in the local coordinate system associated with the interface. Introducing a first-order Taylor-like approximation for the function $\tilde{\boldsymbol{\chi}}(\xi_n, \xi_s, \xi_t)$ in the normal direction $\mathbf{n}$, we write:

$$\tilde{\boldsymbol{\chi}}(\xi_n, \xi_t, \xi_s) = \langle\tilde{\boldsymbol{\chi}}\rangle(\xi_t, \xi_s) + \langle\langle\tilde{\boldsymbol{\chi}}\rangle\rangle(\xi_t, \xi_s)\xi_n + o(\xi_n^2) \tag{22}$$

where $\langle\tilde{\boldsymbol{\chi}}\rangle$ and $\langle\langle\tilde{\boldsymbol{\chi}}\rangle\rangle$ are the thickness averages of the displacement gradients and its normal variation, respectively. Note that the above approximation differs from the standard Taylor series expansion in that the mean displacement gradient and second gradient are used instead of their values at $\xi = 0$. Next, to ensure compatibility between microscopic and macroscopic kinematics, we consider the following relationships:

$$\langle\tilde{\boldsymbol{\chi}}\rangle = \boldsymbol{\Upsilon}_s \quad \text{and} \quad \langle\langle\tilde{\boldsymbol{\chi}}\rangle\rangle = \boldsymbol{\Upsilon}_m/h. \tag{23}$$

In other words, it is assumed that the average of microscopic displacement gradient is equal to the macroscopic displacement gradient introduced in the previous section. This relation provides a natural relationship between microscopic interface deformations and their macroscopic counterparts as follows:

$$\tilde{\boldsymbol{\chi}}(\xi_n, \xi_t, \xi_s) = \boldsymbol{\Upsilon}_s(\xi_t, \xi_s) + \boldsymbol{\Upsilon}_m(\xi_t, \xi_s)\frac{\xi_n}{h} + o(\xi_n^2). \tag{24}$$

In the context of porous media, it is important to estimate changes in macroscopic interface porosity with solid dilation. Dilation at the microscale can be assessed by writing the trace of the displacement gradient $\tilde{e}^v(\xi_n) = tr(\tilde{\boldsymbol{\chi}})$ in the interface. Using (24) and the definition of macroscopic deformation, this yields:

$$\tilde{e}^v(\xi_n, \xi_t, \xi_s) = e_s^v(\xi_t, \xi_s) + e_m^v(\xi_t, \xi_s)\frac{\xi_n}{h} \tag{25}$$

where

$$e_s^v = \frac{[\mathbf{u}]\cdot\mathbf{n}}{h} + tr(\boldsymbol{E}_s^{\parallel}) \quad \text{and} \quad e_m^v = tr(\boldsymbol{\Upsilon}_m) \tag{26}$$

for which the expression of $\boldsymbol{E}_s^{\parallel}$ and $\boldsymbol{\Upsilon}_m$ are given in (16) and (18).

3.1.4. Strain energy and interface stresses

Interface stress measures are now introduced based on energy principles. For this, let us write the elastic energy stored in the medium when the solid phase is subjected to macroscopic deformation $\boldsymbol{E}, [\mathbf{u}], \boldsymbol{E}_s^{\parallel}$ and $\boldsymbol{\Upsilon}_m$. Introducing the elastic energy density ψ in the bulk (per unit volume) and the interface elastic energy density ψ^i (per unit area), the stored elastic energy is written:

$$E_{int} = \int_\Omega \psi dV + \int_\Gamma \psi^i dS. \tag{27}$$

The constitutive relation of the solid is then specified through the relationship between elastic energy densities and strain measures as follows:

$$\psi = \psi(\boldsymbol{E}, p) \quad \text{and} \quad \psi^i = \psi^i([\mathbf{u}], \boldsymbol{E}_s^{\parallel}, \boldsymbol{\Upsilon}_m, \langle p\rangle, [p]) \tag{28}$$

where the independence of ψ and ψ^i on spin measures ensures objectivity (or frame-indifference) of the material behavior. Note that the above relation explicitly shows the dependency of strain energy on interstitial fluid pressure p as well as its average $\langle p\rangle$ and jump $[p]$ across Γ. It is now possible to introduce bulk and interface mixture stresses defined as energy conjugates of the various strains as:

$$\mathbf{T} = \frac{\partial\psi}{\partial\boldsymbol{E}}, \quad \boldsymbol{t}_s = \frac{\partial\psi^i}{\partial[\mathbf{u}]}, \quad \mathbf{T}_s = \frac{\partial\psi^i}{\partial\boldsymbol{E}_s^{\parallel}}, \quad \text{and} \quad \mathbf{T}_m = \frac{\partial\psi^i}{\partial\boldsymbol{\Upsilon}_m}. \tag{29}$$

A physical interpretation for each of these stresses can be given as follows. The quantity $\boldsymbol{t}_s$ represents the cohesive stress between two sides of Γ and contains a component related to interface pressure that tends to open (or close) the interface. The quantity $\mathbf{T}_s$ is the surface stress that arises from the presence of fluid pressure in the interface as well as the resistance of the interface against tangential deformation. It is represented by a symmetric tensor (since $\boldsymbol{E}_s^{\parallel}$ is symmetric). Finally, the tensor $\mathbf{T}_m$ (that is not symmetric) can be interpreted as a couple stress that resists deformation gradients across the interface. With these definitions, a small change in deformation characterized by $\delta\boldsymbol{E}, \delta[\mathbf{u}], \delta\boldsymbol{E}_s^{\parallel}$ and $\delta\,\boldsymbol{\Upsilon}_m$ results in a change of strain energy:

$$\delta E_{int} = \int_\Omega \mathbf{T} : \delta\boldsymbol{E} dV + \int_\Gamma \left(\boldsymbol{t}_s\cdot\delta[\mathbf{u}] + \mathbf{T}_s : \delta\boldsymbol{E}_s^{\parallel} + \mathbf{T}_m : \delta\boldsymbol{\Upsilon}_m\right) dS. \tag{30}$$

The usefulness of this expression will become obvious in Section 4, that concentrates on the derivation of the momentum equations.

3.2. Interstitial fluid flow and driving forces

Besides deformation, the mechanics of fluid-solid mixture is influenced by the motion of a fluid within the porous network and within interfaces. In this context, it is important to note that the present study concentrates on the case of low porosity solids, thin interfaces and relatively large fluid viscosity. This implies that slow Darcy-type fluid flows may be considered. This section introduces an approach to describe bulk and interface fluid flux, based on similar concepts than those introduced for solid deformation. The bases of our description of fluid flow lies in that fluid motion is possible thanks to the existence of thermodynamics driving forces that may have several origins such as gravity, pressure gradients and osmosis, for instance. In general, the origins of the forces can be expressed in terms of a potential function μ, that is denoted as thermodynamic potential in this study. This potential often describes the free energy per unit volume of fluid in terms of mechanical energy (pressure, gravity) and electro-chemical energy (Sun et al., 1999). In this context, the driving force vector $\boldsymbol{\zeta}$ in the bulk is written in terms of the gradient of thermodynamic potential with respect to spatial coordinates:

$$\boldsymbol{\zeta} = -\nabla\mu \tag{31}$$

where the negative sign is due to the fact that by convention, fluid flows in the directions of decreasing μ. In analogy with our previous analysis of solid deformation, it is now possible to define two types of driving forces responsible for fluid flow in Γ, namely, the average driving force $\boldsymbol{\zeta}_s$ and the relative driving force $\boldsymbol{\zeta}_m$.

3.2.1. Mean interface fluid driving force

This thermodynamic force is responsible for fluid motion within the interface and is represented by the average of the fluid driving force on both side of the interface:

$$\boldsymbol{\zeta}_s = -\{\nabla\mu\} \tag{32}$$

The above quantity can generally be decomposed into tangential and normal components as:

$$\boldsymbol{\zeta}_s = \boldsymbol{\zeta}_s^{\parallel} + \zeta_s^{\perp}\,\mathbf{n} \tag{33}$$

where $\boldsymbol{\zeta}_s^{\parallel}$ is the tangential fluid driving force vector and $\zeta_s^{\perp}$ is a scalar that describes the force responsible for fluid flux across Γ. In analogy to interface deformation, tangential component is related to the average bulk driving force, that is projected onto Γ:

$$\boldsymbol{\zeta}_s^{\parallel} = -\mathbf{P}^{\parallel}\cdot\langle\nabla\mu\rangle \tag{34}$$

while the normal component is characterized in terms of the discontinuity in thermodynamic potential μ across Γ:

$$\zeta_s^{\perp} = -[\mu]/h. \tag{35}$$

Here, we note that the factor $1/h$ was used for dimension purposes. However, using similar arguments as for the definition of $\boldsymbol{v}_s^{\perp}$ in (17), the relevant normal driving force will be characterized by the quantity $-[\mu]$ in the remainder of this paper.

3.2.2. Relative interface fluid driving force

The presence of an interface can induce a discontinuity in thermodynamics force at the macroscale which usually results in sharp variation of fluid flux across the interface. To characterize this phenomena, an interface relative fluid driving force ζ_m is introduced as the jump of $\nabla\mu$ across Γ as:

$$\zeta_m = -[\nabla\mu]. \tag{36}$$

This vector can be split into a tangential and normal component $\zeta_m^{\parallel}$ and $\zeta_m^{\perp}$, respectively, such that:

$$\zeta_m = \zeta_m^{\parallel} + \zeta_m^{\perp}\,\mathbf{n}, \tag{37}$$

where

$$\zeta_m^{\parallel} = -\mathbf{P}^{\parallel}\cdot[\nabla\mu] \quad \text{and} \quad \zeta_m^{\perp} = -[\nabla\mu]\cdot\mathbf{n}. \tag{38}$$

The description of thermodynamic forces on the interface is therefore very similar to that of deformation, with the noticeable difference that strains are tensor quantities while thermodynamic forces are vector quantities. In analogy to deformation, one can generally describe fluid flow in the interface in terms of three independent thermodynamic forces: $-[\mu], \zeta_s^{\parallel}$ and ζ_m, which capture discontinuity in thermodynamic potential, mean tangential thermodynamic potential gradient and relative tangential thermodynamic potential gradient, respectively.

3.2.3. Dissipation and fluid velocity

Flow of an interstitial fluid through a solid network is associated with energy dissipation due to fluid viscosity and fluid-solid friction forces (Groenevelt, 2003). It is usually possible to write the total energy dissipation in the solid domain Ω in terms of bulk and interface dissipation potentials φ and φ^i, respectively, measured as dissipation per unit mass of fluid. The total dissipation D arising from interstitial fluid flow is then written:

$$D = \int_{\Omega}\phi\varphi dV + \int_{\Gamma}\bar{\phi}\varphi^i dS. \tag{39}$$

Here φ (and φ^i) represent the amount of dissipated energy in the fluid constituent per unit volume of fluid. They are related to the dissipation per unit mass of fluid $\hat{\varphi}$ (and $\hat{\varphi}^i$) by:

$$\varphi = \rho_t^f\hat{\varphi} \quad \text{and} \quad \varphi^i = \bar{\rho}_t^f\hat{\varphi}^i \tag{40}$$

where ρ_t^f is the true density of the fluid and $\bar{\rho}_t^f$ is the true interface fluid density (that has units of mass per unit area).The constitutive relation for fluid flow in a porous medium is given by the expression of dissipation potentials in terms of thermodynamic driving forces as:

$$\varphi = \varphi(\zeta) \quad \text{and} \quad \varphi^i = \varphi^i([\mu], \zeta_s^{\parallel}, \zeta_m). \tag{41}$$

Because dissipation arises from fictional forces within the solid skeleton, the above equations show a dependency of dissipation potentials on the coordinate $\mathbf{x}$ of a point fixed to the solid phase. Relative fluid velocities (with respect to solid velocities) may then be introduced as energy (dissipation) conjugate of the thermodynamic driving force such that:

$$\mathbf{q} = \frac{\partial\varphi}{\partial\zeta}, \quad q_s^{\perp} = -\frac{\partial\varphi^i}{\partial[\mu]}, \quad \mathbf{q}_s^{\parallel} = \frac{\partial\varphi^i}{\partial\zeta_s^{\parallel}} \quad \text{and} \quad \mathbf{q}_m = \frac{\partial\varphi^i}{\partial\zeta_m} \tag{42}$$

where $\mathbf{q}$ is the relative fluid velocity in the bulk and the three interfacial relative fluid velocities are then representative of the normal relative velocity across the interface ($q_s^{\perp}$), the tangential velocity in the interface $\left(\mathbf{q}_s^{\parallel}\right)$ and the differential velocity between the two sides of the interface ($\mathbf{q}_m$), respectively (Fig. 4). We note that the relative velocity $\mathbf{q}_m$ may be decomposed into a normal and tangential component:

$$\boldsymbol{q}_m = \boldsymbol{q}_m^{\parallel} + q_m^{\perp}\mathbf{n} \tag{43}$$

where $\boldsymbol{q}_m^{\parallel}$ and $q_m^{\perp}$ are derivatives of φ^i with respect to $\zeta_m^{\parallel}$ and $\zeta_m^{\perp}$, respectively. Note that quantities introduced in (42) represent relative fluid velocities with respect to the solid skeleton. In other words, if fluid motion is the same as solid motion, no friction occurs between fluid and solid which results in no dissipation (since all flux vanish). The total dissipation can then be written in terms of the contraction between driving forces and velocities as follows:

$$D = \int_{\Omega}\phi\mathbf{q}\cdot\zeta dV + \int_{\Gamma}\bar{\phi}\left(-q_s^{\perp}[\mu] + \mathbf{q}_s^{\parallel}\cdot\zeta_s^{\parallel} + \mathbf{q}_m\cdot\zeta_m\right)dS. \tag{44}$$

Microscopic fluid velocity in the interface. In order to relate macrocopic and microscopic interface descriptions, let us now consider the velocity $\tilde{\mathbf{q}}(\xi_n, \xi_s, \xi_t)$ (relative to solid motion) in the interface. For small interface thickness h, it is possible to give a linear approximation of $\tilde{\mathbf{q}}$ in the thickness direction $\mathbf{n}$ as:

$$\tilde{\mathbf{q}}(\xi_n, \xi_t, \xi_s) = \langle\tilde{\mathbf{q}}\rangle(\xi_t, \xi_s) + \langle\langle\tilde{\mathbf{q}}\rangle\rangle(\xi_t, \xi_s)\xi_n + o\left(\xi_n^2\right) \tag{45}$$

where the mean velocity $\langle\tilde{\mathbf{q}}\rangle$ and its average normal gradient $\langle\langle\tilde{\mathbf{q}}\rangle\rangle$ are given in (1). Similarly to what was done for solid deformation, averages can be directly related to the macroscopic mean and relative interface velocity by:

$$\langle\tilde{\mathbf{q}}\rangle = \mathbf{q}_s^{\parallel} + q_s^{\perp}\mathbf{n} \quad \text{and} \quad \langle\langle\tilde{\mathbf{q}}\rangle\rangle = \mathbf{q}_m/h. \tag{46}$$

This enables us to write a relation between micro and macroscopic velocities in the form:

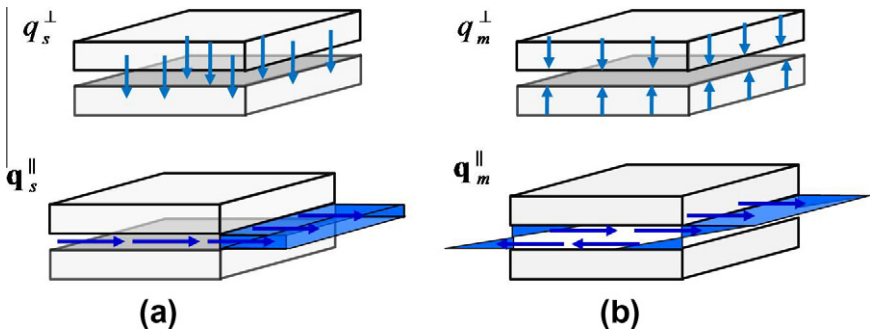

Fig. 4. Representation of macroscopic velocities within the interface. (a) Mean normal and tangential fluid velocities. (b) Normal and tangential relative fluid velocities.

$$\tilde{\mathbf{q}}(\xi_n,\xi_t,\xi_s)=\left(\mathbf{q}_s^{\parallel}+q_s^{\perp}\mathbf{n}\right)(\xi_t,\xi_s)+\mathbf{q}_m(\xi_t,\xi_s)\frac{\xi_n}{h}+o\left(\xi_n^2\right), \tag{47}$$

which will prove useful to explore mass conservation in the interface. Let us now concentrate on the governing equations describing the deformation and fluid flow within a biphasic medium with interfaces. For this, we consider two fundamental principles of continuum mechanics: (a) the conservation of mass and (b) the conservation of momentum.

4. Mass conservation

In order to write the balance of mass in the mixture, it is important to introduce various measures of mass densities in the bulk and in the interface. In the bulk, a particularly useful definition is that of the effective mass density of fluid and solid per unit volume of mixture, given by

$$\rho^f=\phi\rho_t^f \quad \text{and} \quad \rho^s=(1-\phi)\rho_t^s, \tag{48}$$

respectively, where the subscript t denotes the true density of a constituent. Within interfaces, solid densities and porosities may be significantly different from their bulk counterparts. Consistent with our definition of porosities, we consider two macroscopic measures of interface densities $\bar{\rho}^\alpha$ and $\bar{\bar{\rho}}^\alpha$ representing the average mass of constituent α ($\alpha = s,f$) per unit area and its average normal variation within the interface, respectively. They are defined as follows:

$$\bar{\rho}^\alpha=h\langle\tilde{\rho}^\alpha\rangle, \quad \bar{\bar{\rho}}^\alpha=h^2\langle\langle\tilde{\rho}^\alpha\rangle\rangle \tag{49}$$

where the microscopic effective fluid and solid densities are $\tilde{\rho}^f=\tilde{\phi}\tilde{\rho}_t^f$ and $\tilde{\rho}^s=(1-\tilde{\phi})\tilde{\rho}_t^s$ in which the notation $\tilde{\rho}_t^\alpha$ is used for the true density of constituent α. Note that the presence of the interface thickness h in the above equations is necessary so that the interface densities are measures of mass per unit area. To relate microscopic and macroscopic densities, let us now consider a linear approximation of the distribution of mass density across the interface as follows (Fig. 5):

$$\tilde{\rho}^\alpha(\xi_n,\xi_t,\xi_s)=\langle\tilde{\rho}^\alpha\rangle(\xi_t,\xi_s)+\langle\langle\tilde{\rho}^\alpha\rangle\rangle(\xi_t,\xi_s)\xi_n+o\left(\xi_n^2\right) \tag{50}$$

Upon combination with (49), this yields the following microscale-macroscale relation:

$$\tilde{\rho}^\alpha=\frac{1}{h}\bar{\rho}^\alpha+\frac{1}{h^2}\bar{\bar{\rho}}^\alpha\xi_n+o\left(\xi_n^2\right) \tag{51}$$

Next, we propose to derive a set of mass conservation equations for each constituent (fluid and solid) as well as for the entire mixture. The general approach taken in this section consists of first considering microscale mass conservation and use averaging operation to obtain a macroscale representation. The resulting macroscale equations are thus valid under our assumptions regarding the distribution of microscopic densities, deformation and flows given in (51), (24) and (47), respectively.

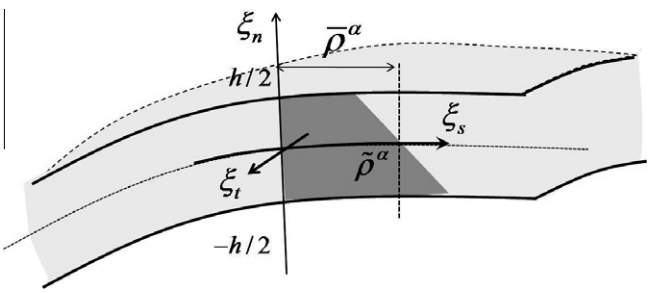

Fig. 5. Microscopic description of the mass density of constituent α in the interface. A linear approximation of densities is assumed between the two sides of the interface.

4.1. Conservation of mass for the solid phase

For each constituent, mass conservation must be explored in two distinct regions: bulk and interface.

4.1.1. Bulk

Following traditional methods, the mass balance in the bulk is established by considering an arbitrary control volume B in Ω that follows the motion of the solid and whose boundary ∂B is chosen in a way such that it does not intersect with interfaces Γ. Fig. 6 depicts such a control volume, for which the boundary is carefully chosen such that it surrounds embedded interfaces. Conservation of mass in B is then written in terms of the material time derivative with respect to solid motion as:

$$\frac{D}{Dt}\int_B\rho^s dV=\int_B\left(\frac{D\rho^s}{Dt}+\rho^s\nabla\cdot\mathbf{v}\right)dV=0, \tag{52}$$

which can be localized to obtain the conventional expression:

$$\frac{D\rho^s}{Dt}+\rho^s\nabla\cdot\mathbf{v}=0. \tag{53}$$

Interface. To derive the mass balance in the interface, we first realize that Eq. (53) also holds for a microscopic point located in the interface at coordinate (ξ_n,ξ_s,ξ_t). We may therefore write:

$$\vartheta(\xi_n,\xi_s,\xi_t)=\frac{D\tilde{\rho}^s}{Dt}+\tilde{\rho}^s\nabla\cdot\tilde{\mathbf{v}}=0. \tag{54}$$

To obtain a macroscopic equation of the mass balance in the interface, it is useful to realize that the above condition can be weakly satisfied at the macroscale if for any values of integer i, the ith moment of ϑ with respect to the normal direction ξ_n vanishes, i.e.:

$$\int_{-h/2}^{h/2}\vartheta(\xi_n,\xi_t,\xi_s)\quad\xi_n^i d\xi_n=0. \tag{55}$$

Physically, each moment equation corresponds to a different level of interface approximation. For instance, if a zeroth order interface model is introduced (the interface density is described by its mean value only), only the zeroth moment equation is needed to characterize mass balance. However, as the order of approximation increases (the density is described with a Taylor approximation of order i), additional equations are needed to enforce macroscopic mass balance. In this case, higher order moment equations (up to order i) are needed. Since the current formulation only considers a first-order approximation of field variation across the interface, the macroscopic mass balance can be derived by invoking the zeroth and first moment equations:

$$\int_{-h/2}^{h/2}\left(\frac{D\tilde{\rho}^s}{Dt}+\tilde{\rho}^s\nabla\cdot\tilde{\mathbf{v}}\right)d\xi_n=0 \tag{56}$$

$$\text{and}\quad\int_{-h/2}^{h/2}\left(\frac{D\tilde{\rho}^s}{Dt}+\tilde{\rho}^s\nabla\cdot\tilde{\mathbf{v}}\right)\xi_n d\xi_n=0. \tag{57}$$

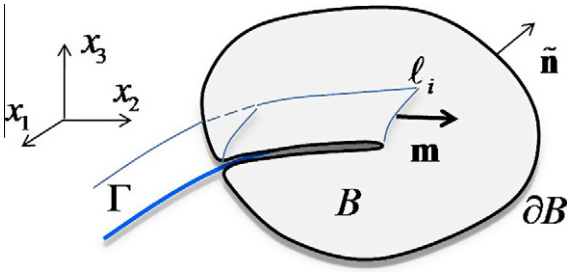

Fig. 6. Control volume B used to derive the mass balance of solid and fluid constituents in the bulk.

Using the fact that $\nabla \cdot \tilde{\mathbf{v}} = \dot{\tilde{e}}^v$ and using the linear approximations (25) and (51) for volumetric deformation and density, we obtain the zeroth and first-order equations for solid mass conservation in the interface:

$$\frac{D\bar{\rho}^s}{Dt} + \bar{\rho}^s \dot{e}^v_s + \bar{\bar{\rho}}^s I \dot{e}^v_m = 0 \tag{58}$$

$$\frac{D\bar{\bar{\rho}}^s}{Dt} + \bar{\bar{\rho}}^s \dot{e}^v_s + \bar{\rho}^s \dot{e}^v_m = 0, \tag{59}$$

where the quantity I is a moment of inertia-like quantity defined as:

$$I = \frac{1}{h^3}\int_{-h/2}^{h/2} \xi_n^2 d\xi^n = \frac{1}{12}.$$

Note that (58) describes the change in interface density $\bar{\rho}^s$ with average volumetric strains, while (59) captures how gradients of volumetric strains across the interface affect the relative solid density $\bar{\bar{\rho}}^s$ in the interface.

4.2. Conservation of mass for the fluid phase

4.2.1. Bulk

Conservation of fluid mass in the bulk is explored by considering the control volume B whose boundary ∂B does not intersect with interfaces as shown in Fig. 6. Using the fact that the motion of a control volume follows that of the solid constituents, mass conservation of the fluid phase can be expressed as follows:

$$\frac{D}{Dt}\int_B \rho^f dV = \int_B \left(\frac{D\rho^f}{Dt} + \rho^f \nabla \cdot \mathbf{v}\right) dV + \int_{\partial B} \rho^f \mathbf{q} \cdot \tilde{\mathbf{n}} dS - \int_{\ell_i} \bar{\rho}^f \mathbf{q}^{\parallel}_s \cdot \mathbf{m} d\ell \tag{60}$$

where $\tilde{\mathbf{n}}$ is the outward unit normal vector to the boundary ∂B of the control volume. The second term in the right-end side is the convective term (written in terms of the relative fluid velocity with respect to solid velocity) and the third term is the velocity entering the domain B through the tip of the interface described by the curve ℓ_i. Note that this curve describes a singularity on the boundary ∂B and is thus considered separately from the other convective terms on ∂B. We also note that the negative sign before the last term is due to the fact that the outward normal $\tilde{\mathbf{n}}$ to the control volume points in the opposite direction of the outward tangential vector $\mathbf{m}$ of the interface. Following (Pouya and Ghabezloo, 2008), the line integral in (60) is replaced by a volume integral using the Dirac delta function to obtain:

$$\int_\ell \bar{\rho}^f \mathbf{q}^{\parallel}_s \cdot \mathbf{m} d\ell = \int_B \bar{\rho}^f \mathbf{q}^{\parallel}_s \cdot \mathbf{m} \delta(\mathbf{x} - \mathbf{x}_{\ell_i}) dV \tag{61}$$

where $\mathbf{x}_{\ell_i}$ denotes the coordinate of points that lie on the curve ℓ_i. Furthermore, applying the divergence theorem to the second term in (60), one can substitute the surface integral by a volume integral, which enables us to localize the equation as follows:

$$\frac{D\rho^f}{Dt} + \rho^f \nabla \cdot \mathbf{v} + \nabla \cdot (\rho^f \mathbf{q}) - \bar{\rho}^f \mathbf{q}^{\parallel}_s \cdot \mathbf{m} \delta(\mathbf{x} - \mathbf{x}_{\ell_i}) = 0. \tag{62}$$

We note that in the above equation, the fluid mass exchange between bulk and the tip of the interface is accounted for by treating the fluid discharge at the tip of the interface as a point source in the bulk (Pouya and Ghabezloo, 2008).

4.2.2. Interface

Concerning mass balance in the interface, we take a similar approach as our analysis of the solid constituent. Starting from the microscopic description of fluid flow, the mass balance equation takes a similar form as (62) (without the term corresponding to the interface discharge):

$$\vartheta(\xi_n, \xi_s, \xi_t) = \frac{D\tilde{\rho}^f}{Dt} + \tilde{\rho}^f \nabla \cdot \tilde{\mathbf{v}} + \nabla \cdot (\tilde{\rho}^f \tilde{\mathbf{q}}) = 0. \tag{63}$$

The equivalent macroscopic equation is found by considering the first and second moment of ϑ as given in (55). This yields the following two equations:

$$\int_{-h/2}^{h/2} \left(\frac{D\tilde{\rho}^f}{Dt} + \tilde{\rho}^f \nabla \cdot \tilde{\mathbf{v}} + \nabla \cdot (\tilde{\rho}^f \tilde{\mathbf{q}})\right) d\xi_n = 0 \tag{64}$$

and

$$\int_{-h/2}^{h/2} \left(\frac{D\tilde{\rho}^f}{Dt} + \tilde{\rho}^f \nabla \cdot \tilde{\mathbf{v}} + \nabla \cdot (\tilde{\rho}^f \tilde{\mathbf{q}})\right) \xi_n d\xi_n = 0. \tag{65}$$

To compute these expressions in terms of macroscopic quantities, the divergence is first decomposed into a normal and tangential term as:

$$\nabla \cdot (\tilde{\rho}^f \tilde{\mathbf{q}}) = \frac{\partial}{\partial \xi_n}(\tilde{\rho}^f \tilde{q}^{\perp}) + div^{\parallel} \cdot (\tilde{\rho}^f \tilde{\mathbf{q}}^{\parallel}) \tag{66}$$

where $\tilde{q}^{\perp}$ and $\mathbf{q}^{\parallel}$ are the normal and tangential projections of the microscopic velocity. Also using the fact that:

$$\int_{-h/2}^{h/2} \frac{\partial}{\partial \xi_n}(\tilde{\rho}^f \tilde{q}_n) d\xi_n = [\rho \mathbf{q} \cdot \mathbf{n}] \tag{67}$$

$$\int_{-h/2}^{h/2} \frac{\partial}{\partial \xi_n}(\tilde{\rho}^f \tilde{q}_n) \xi_n d\xi_n = h\{\rho^f \mathbf{q} \cdot \mathbf{n}\} \bar{\rho}^f q^{\perp}_s - \bar{\bar{\rho}}^f I q^{\perp}_m, \tag{68}$$

substituting the linear approximation for the microscopic fields in (64) and (65) and localizing the integrals, a set of macroscopic equation can be derived as follows:

$$\frac{D\bar{\rho}^f}{Dt} + \bar{\rho}^f \dot{e}^v_s + \bar{\bar{\rho}}^f I \dot{e}^v_m + div^{\parallel}(\bar{\rho}^f \mathbf{q}^{\parallel}_s + \bar{\bar{\rho}}^f I \mathbf{q}^{\parallel}_m) + [\rho^f \mathbf{q} \cdot \mathbf{n}] = 0 \tag{69}$$

$$\frac{D\bar{\bar{\rho}}^f}{Dt} + \bar{\bar{\rho}}^f \dot{e}^v_s + \bar{\rho}^f \dot{e}^v_m + div^{\parallel}(\bar{\bar{\rho}}^f \mathbf{q}^{\parallel}_s + \bar{\rho}^f \mathbf{q}^{\parallel}_m) + \frac{1}{I}\left(\{\rho^f \mathbf{q} \cdot \mathbf{n}\} - \frac{\bar{\rho}^f}{h} q^{\perp}_s - \frac{\bar{\bar{\rho}}^f I}{h} q^{\perp}_m\right) = 0. \tag{70}$$

The first equation describes how changes in interface fluid density is affected by (a) the volumetric deformation of the solid, (b) the tangential velocities $\mathbf{q}^{\parallel}_s$ and $\mathbf{q}^{\parallel}_m$ and (c) the additional normal flux $[\rho^f \mathbf{q} \cdot \mathbf{n}]$ of fluid flowing from the bulk into the interface (or vice-versa). Note that the last term in (69) may also be interpreted as the mass transfer across the interface. The second equation gives additional information on the variation of density across the interface by relating changes in density $\bar{\bar{\rho}}^f$ to interface flux and the mean normal flux $\{\rho^f \mathbf{q} \cdot \mathbf{n}\}$ from the bulk material. It is therefore important to note that the above equations naturally describes the coupling between fluid flow in the bulk and interface.

4.3. Conservation of mass for the mixture and boundary conditions

In many situations, it is relevant to consider the conservation of mass for the entire fluid-solid mixture. Such equations may be derived by adding bulk and interface equations associated with solid constituent ((53), (58), (59)) to those associated with the fluid ((62), (69), (70)). One can therefore show that:

$$\frac{D\rho}{Dt} + \rho \nabla \cdot \mathbf{v} = -div(\rho^f \mathbf{q}) + \bar{\rho}^f \mathbf{q}^{\parallel}_s \cdot \mathbf{m} \delta(\mathbf{x} - \mathbf{x}_{\ell_i}) \tag{71}$$

$$\frac{D\bar{\rho}}{Dt} + \bar{\rho} \dot{e}^v_s + \bar{\bar{\rho}} I \dot{e}^v_m = -div^{\parallel}(\bar{\rho}^f \mathbf{q}^{\parallel}_s + \bar{\bar{\rho}}^f I \mathbf{q}^{\parallel}_m) - [\rho^f \mathbf{q} \cdot \mathbf{n}] \tag{72}$$

$$\frac{D\bar{\bar{\rho}}}{Dt} + \bar{\bar{\rho}} \dot{e}^v_s + \bar{\rho} \dot{e}^v_m = -div^{\parallel}(\bar{\bar{\rho}}^f \mathbf{q}^{\parallel}_s + \bar{\rho}^f \mathbf{q}^{\parallel}_m) - \frac{1}{I}\left(\{\rho^f \mathbf{q} \cdot \mathbf{n}\} - \frac{\bar{\rho}^f}{h} q^{\perp}_s - \frac{\bar{\bar{\rho}}^f I}{h} q^{\perp}_m\right) \tag{73}$$

where we used the fact that the total bulk and interface densities are the sum of the effective density from each phase:

$$\rho = \rho^s + \rho^f, \quad \bar{\rho} = \bar{\rho}^s + \bar{\rho}^f, \quad \bar{\bar{\rho}} = \bar{\bar{\rho}}^s + \bar{\bar{\rho}}^f$$

For the above equations to be solvable, a set of conditions must be prescribed to the boundary $\partial\Omega$ and interface boundary ℓ_e. For this, it is convenient to split $\partial\Omega$ and ℓ_e according to:

$$\partial\Omega = \partial\Omega^q \cap \partial\Omega^\mu \quad \text{and} \quad \ell_e = \ell_e^q \cap \ell_e^\mu$$

for which "fluid velocity" boundary conditions are given on $\partial\,\Omega^q$ and ℓ_e^q while "prescribed thermodynamic potential" boundary conditions are applied on $\partial\Omega^\mu$ and ℓ_e^μ (Fig. 7) as:

$$\begin{aligned} &\mathbf{q}\cdot\mathbf{n} = q \quad \text{on } \partial\Omega^q \quad \text{and} \quad \mu = \bar{\mu} \quad \text{on } \partial\Omega^\mu \\ &\mathbf{q}_s\cdot\mathbf{m} = \bar{q} \quad \text{on } \ell_e^q \quad \text{and} \quad \{\mu\} = \{\bar{\mu}\} \quad \text{on } \ell_e^\mu \\ &\mathbf{q}_m\cdot\mathbf{m} = \bar{\bar{q}} \quad \text{on } \ell_e^q \quad \text{and} \quad [\mu] = [\bar{\mu}] \quad \text{on } \ell_e^\mu \end{aligned} \tag{74}$$

Here q is the prescribed fluid velocity (relative to solid velocity) normal to the boundary $\partial\Omega^q$ while $\bar{q}$ and $\bar{\bar{q}}$ are the prescribed mean and relative interface velocities on the external interface boundaries ℓ_e. Similarly, $\bar{\mu}, \{\bar{\mu}\}$ and $[\bar{\mu}]$ are the prescribed thermodynamic potential, its mean and its jump across ℓ_e, respectively.

4.4. Particular case of incompressible constituents

We now consider the particular case in which both fluid and solid constituents are incompressible, i.e., their true density remains unchanged during material deformation. The incompressibility assumption concerns a large variety of materials, such as gels and soft biological materials at low pressure. Further assuming that true densities are homogeneous across Γ, effective densities can be deduced from porosities $\bar{\phi}$ and $\bar{\bar{\phi}}$ (defined in (2)) using (49):

$$\bar{\rho}^f = h\rho_t^f\bar{\phi}, \quad \bar{\bar{\rho}}^f = h\rho_t^f\bar{\bar{\phi}}, \quad \bar{\rho}^s = h\rho_t^{si}(1-\bar{\phi}) \quad \text{and} \quad \bar{\bar{\rho}}^s = -h\rho_t^{si}\bar{\bar{\phi}} \tag{75}$$

where $\rho_t^{si} = h\tilde{\rho}_t^s$ and $\rho_t^f = h\rho_t^f$. Combining the above expressions with (53), (58), (59), (62), (69) and (70), one can derive the mass balance of the mixture as follows:

$$\nabla\cdot\mathbf{v} + div(\phi\mathbf{q}) - h\bar{\phi}\mathbf{q}_s^{\parallel}\cdot\mathbf{m}\delta(\mathbf{x}-\mathbf{x}_{\ell_i}) = 0 \tag{76}$$

$$\dot{e}_s^v + div^{\parallel}\left(\bar{\phi}\mathbf{q}_s^{\parallel} + \bar{\bar{\phi}}I\mathbf{q}_m^{\parallel}\right) + \frac{[\phi\mathbf{q}\cdot\mathbf{n}]}{h} = 0 \tag{77}$$

$$\dot{e}_m^v + div^{\parallel}\left(\bar{\bar{\phi}}\mathbf{q}_s^{\parallel} + \bar{\phi}\mathbf{q}_m^{\parallel}\right) + \frac{1}{Ih}\left(\langle\phi\mathbf{q}\cdot\mathbf{n}\rangle - \bar{\phi}q_s^{\perp} - \bar{\bar{\phi}}Iq_m^{\perp}\right) = 0. \tag{78}$$

A physical interpretation of each equation is given as follows. The first equation characterizes how the rate of fluid flow equate the rate of solid dilation in the bulk. The equation also shows that fluid mass can be transfered from the interface tip to the bulk (and vice versa) through mean tangential flow $\mathbf{q}_s$. The second equation characterizes the coupling between interface dilation and influx of fluid that may originate from the interface (through $\mathbf{q}_s$ and $\mathbf{q}_m$) and from the bulk (through the term $[\phi\mathbf{q}\cdot\mathbf{n}]$). Finally, the third equation conveys the fact that a difference between the average mass flux $\{\phi\mathbf{q}\cdot\mathbf{n}\}$ across the interface and the normal velocity q_d can arise from a change in relative volumetric strain $\dot{E}_m^v$ or/and from a relative interface velocity (represented by $\bar{\bar{\phi}}\mathbf{q}_s + \bar{\phi}\mathbf{q}_m$). The above equations can be used to determine the relative velocities $\mathbf{v}$, $\mathbf{q}_s$ and $\mathbf{q}_m$ in the bulk and in the interface. In addition, expressions for the evolution of porosities $\phi, \bar{\phi}$ and $\bar{\bar{\phi}}$ is given by the mass conservation of the solid constituents (53), (58) and (59) under the assumption of incompressibility:

$$\frac{D\phi}{Dt} = (1-\phi)\nabla\cdot\mathbf{v} \tag{79}$$

$$\frac{D\bar{\phi}}{Dt} = (1-\bar{\phi})\dot{e}_s^v - I\bar{\bar{\phi}}\dot{e}_m^v \tag{80}$$

$$\frac{D\bar{\bar{\phi}}}{Dt} = -\bar{\bar{\phi}}\dot{e}_s^v + (1-\bar{\phi})\dot{e}_m^v. \tag{81}$$

5. Balance of momentum

To complete the formulation of fluid-solid mixtures with interfaces, we now turn to exploring the macroscopic balance of momentum in the bulk and interfaces.While establishing a relationship between force equilibrium at the microscopic level is a viable strategy to derive equations of momentum balance, we propose to take a different route by invoking the principle of virtual work. This approach has the advantage of using the mathematical formalism of variational calculus to reach the final set of equations with minimal effort. For the sake of simplicity, let us consider the case of a solid under quasi-static conditions, i.e, its motion is slow enough such that inertial forces become negligible compared to other forces, such as fluid pressure and elastic forces. These conditions are typically verified for most applications in soft tissue mechanics and geomechanics. In this context, the principle of virtual work states that the change in mechanical energy in the mixture δE in Ω due to virtual solid displacement is:

$$\delta E = \delta E_{int} - \delta E_{ext} = 0 \tag{82}$$

where δE_{int} denotes the variation of stored elastic energy defined in (30) and δE_{ext} is the variation of work performed by external forces acting on the solid phase. The latter arises from several sources including body forces $\mathbf{b}$, surface traction forces $\mathbf{t}$ on the boundary $\partial\Omega$ and interface tractions $\bar{\mathbf{t}}$ and $\bar{\bar{\mathbf{t}}}$ on the line boundary ℓ_e. Ultimately, the contribution from external forces reads:

$$\delta E_{ext} = \int_\Omega \mathbf{b}\cdot\delta\mathbf{u}dV + \int_{\partial\Omega^t}\mathbf{t}\cdot\delta\mathbf{u}dS + \int_{\ell_e^t}\left(\bar{\mathbf{t}}\cdot\delta\{\mathbf{u}\} + \bar{\bar{\mathbf{t}}}\cdot\delta[\mathbf{u}]\right)d\ell. \tag{83}$$

Physically, $\bar{\mathbf{t}}$ and $\bar{\bar{\mathbf{t}}}$ represent the average tension and the jump in tension on the intersection of the interface and the body's boundary. To describe the boundary conditions, domain boundaries are decomposed in two parts as:

$$\partial\Omega = \partial\Omega^t \cap \partial\Omega^u \quad \text{and} \quad \ell_e = \ell_e^t \cap \ell_e^u$$

where "traction" boundary conditions are applied on $\partial\,\Omega^t$ and ℓ_e^t and "prescribed displacement" boundary conditions are applied on $\partial\Omega^u$ and ℓ_e^u. To derive the governing differential equations of momentum balance, we start by integrating (30) by parts and

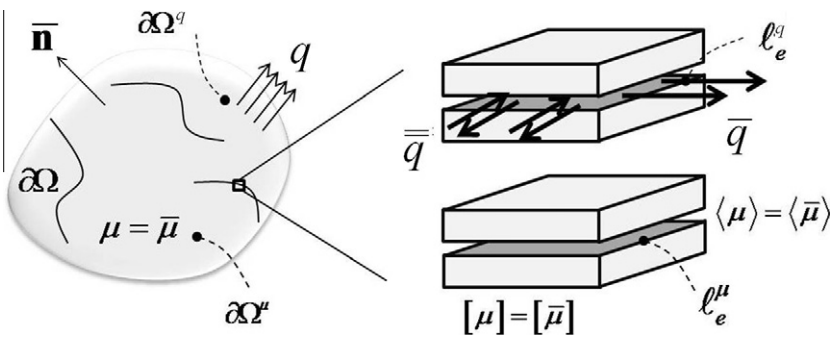

Fig. 7. Various types of fluid velocity boundary conditions associated with bulk and interface.

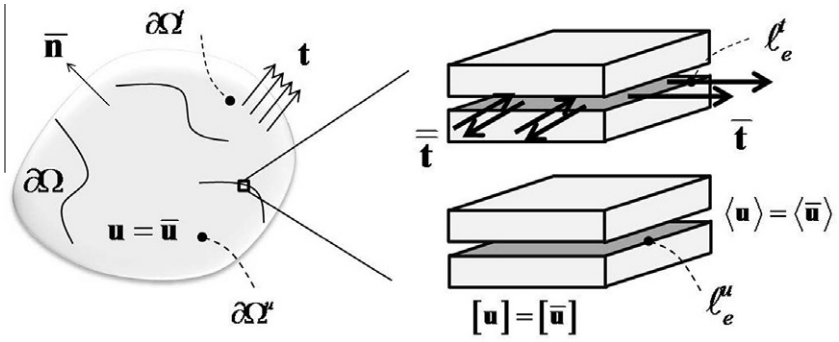

Fig. 8. Traction and displacement boundary conditions associated with bulk and interface.

applying the divergence theorem. This leads to an alternative expression of the variation of internal energy:

$$\begin{aligned}\delta E_{int} = &-\int_\Omega div\mathbf{T}\cdot\delta\mathbf{u}dV+\int_\Gamma(\boldsymbol{t}_s\cdot\delta[\![\mathbf{u}]\!]-div^{\parallel}\mathbf{T}_s\cdot\delta\{\mathbf{u}\}\\&-div^{\parallel}\mathbf{T}_m\cdot\delta[\![\mathbf{u}]\!])dS-\int_\Gamma[(\mathbf{T}\cdot\mathbf{n})\cdot\delta\mathbf{u}]dS+\int_{\partial\Omega}(\mathbf{T}\cdot\bar{\mathbf{n}})\cdot\delta\mathbf{u}dS\\&+\int_{\ell_i}(\mathbf{T}_s\cdot\mathbf{m})\cdot\delta\mathbf{u}d\ell+\int_{\ell_e}((\mathbf{T}_s\cdot\mathbf{m})\cdot\delta\{\mathbf{u}\}+(\mathbf{T}_m\cdot\mathbf{m})\cdot\delta[\![\mathbf{u}]\!])d\ell\end{aligned}\quad(84)$$

where $\bar{\mathbf{n}}$ is the unit vector normal to the boundary $\partial\Omega$ and $\mathbf{m}$ is the unit vector that is tangent to interface Γ. Here, we used the fact that the discontinuity in displacement vanishes at the interface boundary (when it does not intersect with $\partial\Omega$). In other words, we enforced the condition $[\![\mathbf{u}]\!]=0$ and $\{\mathbf{u}\}=\mathbf{u}$ on ℓ_i. Furthermore, using the fact that,

$$[(\mathbf{T}\cdot\mathbf{n})\cdot\delta\mathbf{u}]=[\mathbf{T}\cdot\mathbf{n}]\cdot\{\delta\mathbf{u}\}+\{\mathbf{T}\cdot\mathbf{n}\}\cdot[\![\delta\mathbf{u}]\!]\quad(85)$$

and realizing that:

$$\int_{\ell_i}(\mathbf{T}_s\cdot\mathbf{m})\cdot\delta\mathbf{u}d\ell=\int_\Omega(\mathbf{T}_s\cdot\mathbf{m})\delta(\mathbf{x}-\mathbf{x}_{\ell_i})\cdot\delta\mathbf{u}dV\quad(86)$$

where $\delta(\mathbf{x}-\mathbf{x}_{\ell_i})$ is the Dirac delta function, the quantity δE_{int} can be rewritten in the more convenient form:

$$\begin{aligned}\delta E_{int} = &\int_\Omega(-div\mathbf{T}+(\mathbf{T}_s\cdot\mathbf{m})\delta(\mathbf{x}-\mathbf{x}_{\ell_i}))\cdot\delta\mathbf{u}dV\\&+\int_\Gamma\left(\boldsymbol{t}_s-div^{\parallel}\mathbf{T}_m-\{\mathbf{T}\cdot\mathbf{n}\}\right)\cdot\delta[\![\mathbf{u}]\!]+(-div^{\parallel}\mathbf{T}_s\\&-[\mathbf{T}\cdot\mathbf{n}])\cdot\delta\{\mathbf{u}\}dS+\int_{\partial\Omega}(\mathbf{T}\cdot\mathbf{n})\cdot\delta\mathbf{u}dS\\&+\int_{\ell_e}((\mathbf{T}_s\cdot\mathbf{m})\cdot\delta\langle\mathbf{u}\rangle+(\mathbf{T}_m\cdot\mathbf{m})\cdot\delta[\![\mathbf{u}]\!])d\ell.\end{aligned}\quad(87)$$

It is now possible to substitute (87) and (83) into (82) to obtain an suitable integral form of the principle of virtual work. Using the fact that the expression is true for any arbitrary fields $\delta\mathbf{u}$, $\{\delta\mathbf{u}\}$ and $[\![\delta\mathbf{u}]\!]$ that satisfy the following conditions on the Dirichlet boundaries:

$$\delta u=0\quad\text{on }\partial\Omega^u,\quad\delta[\![u]\!]=0\quad\text{on }\ell_e^u\quad\text{and}\quad\delta\{u\}=0\quad\text{on }\ell_e^u,$$

the following differential equations can be obtained:

$$div\mathbf{T}+\mathbf{b}-(\mathbf{T}_s\cdot\mathbf{m})\delta(\mathbf{x}-\mathbf{x}_{\ell_i})=0\quad\text{in }\Omega\quad(88)$$

$$div^{\parallel}\mathbf{T}_s+[\![\mathbf{T}\cdot\mathbf{n}]\!]=0\quad\text{on }\Gamma\quad(89)$$

$$div^{\parallel}\mathbf{T}_m+\{\mathbf{T}\cdot\mathbf{n}\}-\boldsymbol{t}_s=0\quad\text{on }\Gamma.\quad(90)$$

We also find that the above equations are complemented by boundary conditions in the form (Fig. 8):

$$\begin{aligned}&\mathbf{T}\cdot\mathbf{n}=\mathbf{t}\quad\text{on }\partial\Omega^t\quad\text{and}\quad\mathbf{u}=\bar{\mathbf{u}}\quad\text{on }\partial\Omega^u\\&\mathbf{T}_s\cdot\mathbf{m}=\bar{\mathbf{t}}\quad\text{on }\ell_e^t\quad\text{and}\quad\{\mathbf{u}\}=\{\bar{\mathbf{u}}\}\quad\text{on }\ell_e^u\\&\mathbf{T}_m\cdot\mathbf{m}=\bar{\bar{\mathbf{t}}}\quad\text{on }\ell_e^t\quad\text{and}\quad[\![\mathbf{u}]\!]=[\![\bar{\mathbf{u}}]\!]\quad\text{on }\ell_e^u\end{aligned}\quad(91)$$

where $\bar{\mathbf{u}}$, $\{\bar{\mathbf{u}}\}$ and $[\![\bar{\mathbf{u}}]\!]$ are prescribed solid displacements on the domain and interface external boundaries. Eq. (88) represents force equilibrium in the bulk, in which the effect of interface tension at the interface boundary appears through the term $\left(\mathbf{T}_s^{\parallel}\cdot\mathbf{m}\right)\delta(\mathbf{x}-\mathbf{x}_{\ell_i})$ (Fig. 9a). Thus, surface tension on interfaces may be interpreted as an equivalent concentrated tangential force located at the edge of interfaces. Interface equilibrium is represented by (89) and (90). To fully apprehend their physical meaning, the forces acting on the interface are decomposed into an average stress (that tends to generate relative deformation on each side of the interface) and stress discontinuity (that is associated with interface tension). As shown in Fig. 9b, the average stress generates a cohesive stress $\boldsymbol{t}_s$ and a differential stress distribution within the interface, represented by $\mathbf{T}_m$. The equilibrium between these stress components is given by (89). In addition, the presence of a stress discontinuity across Γ is compensated by a surface stress T_s, acting along the surface tangent (Fig. 9c). This effect is represented by (90) and may be compared with the Laplace-Young relation for surface tension on the free-surface of fluids. In solids, this effect plays an important role at the nano-scale, where surface tension becomes dominant (Farsad et al., 2010).

6. Constitutive relations

We now need to postulate the constitutive relationship between bulk/interface stress and deformation as well as bulk/interface velocity and thermodynamic forces. Restricting ourselves to the simple case of linear relationships, the constitutive relation is given in terms of scalar functions describing the strain energy functions and dissipation potentials in the bulk and the interface. The particular case of isotropic bulk and interfaces is then explored.

6.1. Elasticity of the solid phase

As suggested by Eq. (29), the constitutive relation describing the deformation of the solid phase is entirely defined by the strain energy functions ψ and ψ^i. To ensure positive-definite material stiffness, strain energies must be convex functions of the strain measures in the bulk and interface. For small strains, this condition is satisfied by introducing a quadratic function in the form:

$$\psi=\psi^0+\mathbf{T}^0:\boldsymbol{E}+\frac{1}{2}\boldsymbol{E}:\mathbf{C}:\boldsymbol{E}\quad(92)$$

where ψ^0 is the initial energy (per unit material volume) stored in the medium when it is unstrained, $\mathbf{T}^0$ is the pre-stress and $\mathbf{C}$ is

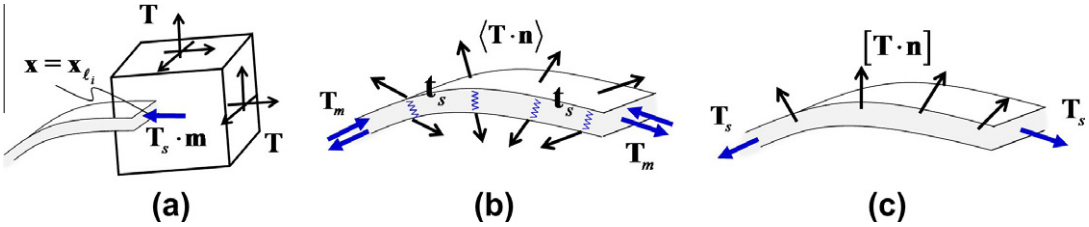

Fig. 9. Physical interpretation of bulk and interface equilibrium equations for the solid phase.

the symmetric, positive-definite, fourth-order elasticity tensor. Similarly, on Γ, the elastic energy (per unit interface area) is written as a quadratic form of the various interface deformation measures as follows:

$$\begin{aligned}\psi_i^0 = \psi_i^0 + \mathbf{t}_s^0 \cdot [\mathbf{u}] + \mathbf{T}_s^0 : \boldsymbol{E}_s^{\parallel} + \mathbf{T}_m^0 : \boldsymbol{\Upsilon}_m + \frac{1}{2}[\mathbf{u}] \cdot \mathbf{C}_d \cdot [\mathbf{u}] + \frac{1}{2}\boldsymbol{E}_s^{\parallel} \\ : \mathbf{C}_s : \boldsymbol{E}_s^{\parallel} + \frac{1}{2}\boldsymbol{\Upsilon}_m : \mathbf{C}_m : \boldsymbol{\Upsilon}_m + [\mathbf{u}] \cdot \mathbf{C}_{ds} : \boldsymbol{E}_s^{\parallel} + [\mathbf{u}] \cdot \mathbf{C}_{dm} \\ : \boldsymbol{\Upsilon}_m + \boldsymbol{\Upsilon}_m : \mathbf{C}_{sm} : \boldsymbol{E}_s^{\parallel}.\end{aligned} \tag{93}$$

Here ψ_i^0 is the initial energy in the interface and $\boldsymbol{t}_s^0, \mathbf{T}_s^0$ and $\mathbf{T}_m^0$ are the initial cohesive stress in the interface, the tangential interface prestress and initial interface stress couple, respectively. In addition, $\mathbf{C}_d$ is a second-order tensor representing the cohesive stiffness of the interface, $\mathbf{C}_s$ is a fourth-order tensor representing the stiffness of the interface in the tangential plane and $\mathbf{C}_m$ (also a fourth-order tensor) characterizes the resistance against the development of strain gradients across Γ. Finally, $\mathbf{C}_{ds}$, $\mathbf{C}_{dm}$ and $\mathbf{C}_{sm}$ are elastic matrices that characterize interactions between different modes of interface deformation. For instance, $\mathbf{C}_{ds}$ captures the variation of surface stress with decohesion (and vice-versa). Using (29), the stress-strain relationship can then be written in the form:

$$\mathbf{T} = \mathbf{T}^0 + \mathbf{C} : \boldsymbol{E} \tag{94}$$

$$\boldsymbol{t}_s = \mathbf{t}_s^0 + \mathbf{C}_d \cdot [\mathbf{u}] + \mathbf{C}_{ds} : \boldsymbol{E}_s^{\parallel} + \mathbf{C}_{dm} : \boldsymbol{\Upsilon}_m \tag{95}$$

$$\mathbf{T}_s = \mathbf{T}_s^0 + \mathbf{C}_{ds} \cdot [\mathbf{u}] + \mathbf{C}_s : \boldsymbol{E}_s^{\parallel} + \mathbf{C}_{sm} : \boldsymbol{\Upsilon}_m \tag{96}$$

$$\mathbf{T}_m = \mathbf{T}_m^0 + \mathbf{C}_{dm} \cdot [\mathbf{u}] + \mathbf{C}_{sm} : \boldsymbol{E}_s^{\parallel} + \mathbf{C}_m : \boldsymbol{\Upsilon}_m. \tag{97}$$

For biphasic media, the mechanical interaction between fluid and solid is traditionally described by the effective stress principle, that relates initial stress in the bulk to the interstitial fluid pressure p by:

$$\mathbf{T}^0 = -p\mathbf{I} \tag{98}$$

where the negative sign is due to different conventions regarding the pressure definition in fluid and solid. For instance, a compressive state leads to a positive hydrostatic fluid pressure but a negative hydrostatic stress in the solid. It is also interesting to note that (98), together with (94) and (88) describe the classical steady state poroelasticity equations (including a non-homogeneous terms arising from the existence of $\mathbf{T}_s$). Extending the effective stress principle to the interface, we write:

$$\mathbf{t}_s^0 = -p^i\mathbf{n} \quad \mathbf{T}_s^0 = -\{p\}\mathbf{P}^{\parallel} \cdot \mathbf{P}^{\parallel} \quad \text{and} \quad \mathbf{T}_m^0 = -[p]\mathbf{P}^{\parallel} \cdot \mathbf{P}^{\parallel} \tag{99}$$

where $\{p\}$ and $[p]$ are the average pressure and pressure discontinuity across the interface, respectively. In the above expressions, the first equality describes the appearance of a normal cohesive stress with interface fluid pressure; this may contribute to interface openings as pressure increases, for instance. The second equality characterizes the existence of an interfacial tangential stress with internal pressure that results in interface extension with increasing internal pressure. This phenomena may be compared to the surface tension in bi-materials interfaces at the nano-scale (Farsad et al., 2010). Finally, the third equality describes the existence of a stress couple $\mathbf{T}_m^0$ when fluid pressure differs on each side of Γ.

6.2. Dissipation in the fluid phase

Constitutive relations for fluid flow follows from the definition of convex dissipation potentials φ and φ_i as introduced in (41). In the bulk, one can consider a quadratic function in the form:

$$\varphi = \varphi^0 + \mathbf{q}^0 \cdot \boldsymbol{\zeta} + \frac{1}{2}\boldsymbol{\zeta} \cdot \boldsymbol{\kappa} \cdot \boldsymbol{\zeta} \tag{100}$$

where $\boldsymbol{\zeta}$ was defined in (31) and φ^0 represents the dissipation from processes other than fluid flow, $\mathbf{q}^0$ is interpreted as an initial velocity per unit volume in the medium and $\boldsymbol{\kappa}$ represents the ratio of solid permeability and fluid viscosity. On the interface, the dissipation per unit area is written:

$$\begin{aligned}\varphi_i = &\varphi_i^0 - q_s^{\perp 0}[\mu] + \mathbf{q}_s^{\parallel 0} \cdot \boldsymbol{\zeta}_s^{\parallel} + \mathbf{q}_m^0 \cdot \boldsymbol{\zeta}_m + \frac{1}{2}\kappa_s^{\perp}[\mu]^2 + \frac{1}{2}\boldsymbol{\zeta}_s^{\parallel} \cdot \boldsymbol{\kappa}_s \cdot \boldsymbol{\zeta}_s^{\parallel} \\ &+ \frac{1}{2}\boldsymbol{\zeta}_m \cdot \boldsymbol{\kappa}_m \cdot \boldsymbol{\zeta}_m - [\mu]\boldsymbol{\kappa}_{ds} \cdot \boldsymbol{\zeta}_s^{\parallel} - [\mu]\boldsymbol{\kappa}_{dm} \cdot \boldsymbol{\zeta}_m + \boldsymbol{\zeta}_s^{\parallel} \cdot \boldsymbol{\kappa}_{sm} \cdot \boldsymbol{\zeta}_m\end{aligned} \tag{101}$$

where we introduced the flux-independent dissipation φ_i^0, and the interface initial velocities $q_s^{\perp 0}, \mathbf{q}_s^0$, and $\mathbf{q}_m^0$ that may arise from the existence of *pumps* on the interface. For instance, this situation may arise on biological cell membranes, in which ATP pumps can produce outward or inward flux q_d^0 into the cell (Alberts et al., 2002). Expression (41) also introduced measures of average interface permeabilities κ_d (scalar) and $\boldsymbol{\kappa}_s$ (second-order tensor) in the normal and tangential directions, respectively, as well as the permittance of differential flow in the interface is given by $\boldsymbol{\kappa}_m$. Finally, matrices $\boldsymbol{\kappa}_{ds}$, $\boldsymbol{\kappa}_{dm}$ and $\boldsymbol{\kappa}_{sm}$ describe the interactions between various modes of interface flux; such interaction typically occur for anisotropic or inhomogeneous interfaces. The definition of the above dissipation potential enables us to relate fluid velocities and thermodynamic forces using (42):

$$\mathbf{q} = \mathbf{q}^0 + \boldsymbol{\kappa} \cdot \boldsymbol{\zeta} \tag{102}$$

$$q_s^{\perp} = q_s^{\perp 0} - \kappa_s^{\perp}[\mu] + \boldsymbol{\kappa}_{ds} \cdot \boldsymbol{\zeta}_s^{\parallel} + \boldsymbol{\kappa}_{dm} \cdot \boldsymbol{\zeta}_m \tag{103}$$

$$\mathbf{q}_s^{\parallel} = \mathbf{q}_s^{\parallel 0} - \boldsymbol{\kappa}_{ds}[\mu] + \boldsymbol{\kappa}_s \cdot \boldsymbol{\zeta}_s^{\parallel} + \boldsymbol{\kappa}_{sm} \cdot \boldsymbol{\zeta}_m \tag{104}$$

$$\mathbf{q}_m = \mathbf{q}_m^0 - \boldsymbol{\kappa}_{dm}[\mu] + \boldsymbol{\kappa}_{sm} \cdot \boldsymbol{\zeta}_s^{\parallel} + \boldsymbol{\kappa}_m \cdot \boldsymbol{\zeta}_m \tag{105}$$

We note that the first equation is the conventional Darcy's law for the flow of a fluid in a porous medium. Flux within the interface are then specified through linear relations with thermodynamic forces. Because the constitutive relation is derived from a dissipation potential, symmetry is observed regarding the interaction terms $\boldsymbol{\kappa}_{ds}$, $\boldsymbol{\kappa}_{dm}$, and $\boldsymbol{\kappa}_{sm}$. The proposed formulation therefore automatically verifies the Onsager principle (Groenevelt, 2003) for fluid flow in the interface.

6.3. Special case of an isotropic and uncoupled interface

We now restrict our attention to interfaces that are isotropic in the plane, i.e, their properties are unchanged under any rotation

about the normal vector $\mathbf{n}$. Furthermore, we assume that the modes of interface deformation are totally uncoupled (interaction terms vanish), an assumption that is valid for the small deformation of microscopically homogeneous interfaces. Finally, we assume that the strain energy depends on the tangential relative strain $\Upsilon_m^{\parallel}$ but is independent of the relative normal strain $\upsilon_m^{\perp}$. In this case, Eqs. (95)–(97) become:

$$\boldsymbol{t}_s = -p^i\mathbf{n} + \mathbf{C}_d \cdot [\mathbf{u}] \tag{106}$$

$$\mathbf{T}_s = -\{p\}\mathbf{P}^{\parallel} \cdot \mathbf{P}^{\parallel} + \mathbf{C}_s : \boldsymbol{E}_s^{\parallel} \tag{107}$$

$$\mathbf{T}_m = -[p]\mathbf{P}^{\parallel} \cdot \mathbf{P}^{\parallel} + \mathbf{C}_m^E : \boldsymbol{E}_m^{\parallel} + \mathbf{C}_m^w : \boldsymbol{W}_m^{\parallel} \tag{108}$$

where we decomposed the matrix $\mathbf{C}_m$ into a component $\mathbf{C}_m^E$ acting on the relative strain $\boldsymbol{E}_m$ and a component $\mathbf{C}_m^w$ acting on the relative spin $\boldsymbol{W}_m$. Taking advantage of the isotropy, the constitutive relation can be reduced to the knowledge of seven material constants as follows:

$$C_{d,ij} = k_d^n n_i n_j + k_d^s P_{ij}^{\parallel} \tag{109}$$

$$C_{s,ijkl} = \lambda_s P_{ij}^{\parallel} P_{kl}^{\parallel} + \mu_s \left(P_{ik}^{\parallel} P_{jl}^{\parallel} + P_{il}^{\parallel} P_{jk}^{\parallel} \right) \tag{110}$$

$$C_{m,ijkl}^E = \lambda_m P_{ij}^{\parallel} P_{kl}^{\parallel} + \mu_m \left(P_{ik}^{\parallel} P_{jl}^{\parallel} + P_{il}^{\parallel} P_{jk}^{\parallel} \right) \tag{111}$$

$$C_{m,ijkl}^w = \mu_m^w \left(P_{ik}^{\parallel} P_{jl}^{\parallel} + P_{il}^{\parallel} P_{jk}^{\parallel} \right). \tag{112}$$

Here, k_d^n and k_d^s denote the cohesive stiffness in the normal and tangential directions, respectively while λ_s and μ_s are the lame constants associated with the tangential deformation of the interface. In addition, stiffness related to relative strain are represented by λ_m and μ_m while the resistance to spin discontinuity across the interface arise from the modulus μ_m^w.

The specification of interstitial fluid flow depends on the definition of the potential μ from which the thermodynamical forces are derived. While this function may comprise a variety of terms that characterize mechanical, chemical and electrical contributions to fluid motion, we focus here on the particular case in which fluid flow is affected by two factors: interstitial fluid pressure and gravitational forces. This means that the function μ is written as:

$$\mu = \mu_0 + p + \rho_t^f g z \tag{113}$$

where μ_0 is the reference potential, ρ_t^f is the true fluid density, g is the gravitational constant and z is the vertical coordinate in an arbitrary Cartesian coordinate system. The expression for the relative velocity $\mathbf{q}$ in the bulk automatically follows from (31), (102) and (113) and take the form of the classical Darcy's law as:

$$\mathbf{q} = -\kappa \left(\nabla p + \rho_t^f g \mathbf{k} \right) \tag{114}$$

where the scalar κ represents the ratio of isotropic permeability and fluid viscosity in the bulk.

Furthermore, for an uncoupled interface, interaction terms $\boldsymbol{\kappa}_{ds}$, $\boldsymbol{\kappa}_{dm}$ and $\boldsymbol{\kappa}_{sm}$ vanish and using the condition of isotropy, interface permeabilities $\boldsymbol{\kappa}_s$ and $\boldsymbol{\kappa}_m$ are reduced to scalar quantities κ_s and κ_m. Using (103)–(105), together with 35, 34, 36 and 113, the constitutive relation fluid flow in Γ becomes:

$$q_s^{\perp} = -\kappa_s^{\perp}[p] \tag{115}$$

$$\mathbf{q}_s^{\parallel} = -\kappa_s^{\parallel}\mathbf{P}^{\parallel} \cdot (\{\nabla p\} + g\mathbf{k}) \tag{116}$$

$$\mathbf{q}_m = -\boldsymbol{\kappa}_m[\nabla p] \tag{117}$$

where it is implicitly assumed that there are no pre-flux in the interface. Note that in the case of a horizontal interface, the quantity $\mathbf{P}^{\parallel} \cdot \mathbf{k}$ vanishes, and gravity has no effect on fluid flow within Γ. Also, in the case where $\kappa_s^{\perp} = 0$, the interface becomes impermeable, i.e, no fluid can cross Γ. Alternatively, if $\kappa_s^{\parallel} = 0$, no mean tangential flux is allowed.

7. Discussion and conclusion

The objective of this paper was to explore the mechanical behavior of interfaces in saturated fluid-solid mixtures. Under the assumption of small deformations, we have shown that the mechanics of the mixture with embedded interfaces can be described by two independent fields: the solid displacement field $\mathbf{u}$ and the potential energy of the fluid phase μ that are continuous within the bulk and discontinuous across interfaces. With the knowledge of these fields, we have shown that the deformation and flux within the interface could be characterized in terms of various measures of interface strain and fluid driving force, defined as projections of bulk quantities onto the interface. In particular, it was possible to consider interface deformations such as decohesion, tangential strain and relative tangential strains, and characterize interface fluid flux in terms normal flow, mean tangential flow and relative tangential flow, respectively.

Governing equations for the fluid-solid mixture were then derived by explofring mass conservation and the balance of momentum. This led to a coupled system of partial differential equations describing the interaction between solid deformation and fluid flow in both bulk and interfaces. It is important to mention that the proposed formulation is accurate for interface thicknesses that are small enough such that strain fields and fluid flux vary linearly across the thickness. In the case where interface thickness becomes too large, alternative formulations, coupling Stokes equations with Darcy's law have been proposed (Bernardi et al., 2008). According to interface thickness, it is interesting to note that the proposed formulation allows for several level of approximations. In the most general formulation, the behavior of interfaces in porous media (with incompressible constituents) is described by governing Eqs. (76)–(78) together with stress Eqs. (88)–(90). However, in the case where interfaces are infinitesimally thin, fields such as porosity, strain and flux cannot vary across the interface thickness and relative deformation Υ_m, flux $\mathbf{q}_m$ and porosity $\bar{\phi}$ are negligible according to 24, 47 and 51. In this situation, it is straightforward to show that by simplifying (77) and (78), a reduced set of interface equations for mass conservation and momentum balance can be obtained as follows:

$$\begin{aligned} &\dot{e}_s^v + div^{\parallel}(\bar{\phi}\mathbf{q}_s) + [\phi\mathbf{q}\cdot\mathbf{n}]/h = 0 \quad div^{\parallel}\mathbf{T}_s + [\mathbf{T}\cdot\mathbf{n}] = 0 \\ &\{\phi\mathbf{q}\cdot\mathbf{n}\} - \bar{\phi}q_s^{\perp} = 0 \quad \{\mathbf{T}\cdot\mathbf{n}\} - \boldsymbol{t}_s = 0. \end{aligned} \tag{118}$$

These equations are complemented by the porosity evolution equation arising from (80):

$$\frac{D\bar{\phi}}{Dt} = (1-\bar{\phi})\dot{e}_s^v. \tag{119}$$

This simplified formulation may be attractive for a variety of applications due to its simpler nature and reasonable accuracy. Indeed, despite of the simplification, key phenomena such as mean interface flow as well as interface decohesion and interface tension are still accounted for. It is also of interest to consider the case in which the interface disappears (i.e. $h = 0$). In this case, all tangential fields vanish and the governing equations of the interface reduce to:

$$\begin{aligned} &[\mathbf{q}\cdot\mathbf{n}] = 0 \quad [\mathbf{T}\cdot\mathbf{n}] = 0 \\ &\{\mathbf{q}\cdot\mathbf{n}\} - q_s^{\perp} = 0 \quad \{\mathbf{T}\cdot\mathbf{n}\} - \boldsymbol{t}_s = 0 \end{aligned} \tag{120}$$

where it was assumed that there was no discontinuity in porosity ϕ across the interface. It is clear that the above equations ensure that stress and flux are continuous across Γ, a feature that is expected when no physical interfaces are present. In other words, the proposed formulation degenerates to the conventional theory of mixture without interface.

Finally, a linear elastic constitutive relation and linear relationship between flow and driving forces was considered. In the most

general case, the interface response is described in terms of a large number of elastic constants for deformation and permeabilities characterizing a wide variety of phenomena occurring at the interface. However, we showed that by considering the simple case of isotropic, uncoupled interfaces, the constitutive response could be reduced to only five elastic constants and three permeabilities, making the proposed formulation more tractable. Although we only considered the case in which the fluid potential energy depends on gravity and pressure, the formulation can easily be extended to more complex situations in which chemical energies become more significant (Sun et al., 1999).

In summary, the results presented in this paper are important to characterize the macroscopic behavior of hydrated materials with embedded interfaces, such as bio-materials, soils or hydrogels, to name a few. Accurate constitutive relations at the scale of the interface may be derived using homogenization techniques (Bayada and Chambat, 1995) that were briefly addressed in this paper through the micro-macro approach. The proposed theory may then be used to solve multiscale problems in which large domains are needed in conjunction with fine interface descriptions (Vernerey et al., 2007a; Vernerey et al., 2007b). For such complex problems, the derived equations can be naturally solved with numerical methods such as the extended finite element method, accounting for discontinuities across interfaces and coupled with the levelset method to describe the geometry of interfaces (Farsad et al., 2010). Future research activities will therefore consist in deriving material constants from homogenization techniques as well as deriving a numerical strategy to obtain a solution of the proposed formulation for the general case of curved interfaces in elastic bodies. The extension of the formulation to the case of large deformation and rotation is also of great interest in the context of soft biological tissues.

Acknowledgment

Discussions with R. Pak are gratefully acknowledged. The author would also like to thank the National Science Foundation, Grant No. CMMI-0900607 in support for this work.

References

Alberts, B., Johnson, A.A.L., Raff, M., Roberts, K., Walter, P., 2002. Molecular Biology of the Cell, fourth ed. Garland Science, Taylor and Francis, New York.

Barthelemy, J., 2009. Effective permeability of media with a dense network of long and micro fractures. Transport in Porous Media 76, 153–178.

Bayada, G., Chambat, M., 1995. On interface conditions for a thin film flow past a porous medium. Journal on Mathematical Analysis, 26, pp. 1113–1129.

Bernardi, C., Hecht, F., Pironneau, O., 2008. Coupling darcy and stokes equations for porous media with cracks. Mathematical Modelling and Numerical Analysis 39, 7–35.

Biot, M., 1941. General theory of three-dimensional consolidation. Journal of Applied Physics 12, 155–164.

Biot, M., 1957. The elastic coefficients of the theory of consolidation. Journal of Astrophysics and Astronomy 24, 594–601.

Bowen, R., 1980. Incompressible porous media models by the use of the theory of mixtures. International Journal of Engineering Science 18, 1129–1148.

Dormieux, L., Kondo, D., 2007. Approche micromecanique du couplage permeabilite-endommagement. C.R. Mecanique 332, 135–140.

Farsad, M., Vernerey, F., Park, H., 2010. An extended finite element/level set method to study surface effects on the mechanical behavior and properties of nanomaterials. International Journal for Numerical Methods in Engineering 84, 1466–1489.

Ghabezloo, S., Pouya, A., 2008. Numerical upscaling of the permeability of a randomly cracked porous medium. In: The 12th International Conference of International Association for Computer Methods and Advances in Geomechanics (IACMAG).

Groenevelt, P., 2003. The place of darcy's law in the framework of non-equilibrium thermodynamics. Henry P.G. Darcy and other pioneers in hydraulics: contributions in Celebration of the 200th Birthday of Henry Philibert Gaspard Darcy , pp. 71–77.

Gurtin, M., Weissmuller, J., Larche, F., 1998. A general theory of curved deformable interfaces in solids at equilibrium. Philosophical Magazine A 78, 1093–1109.

Liolios, P., Exadaktylos, G., 2008. A solution of steady-state fluid flow in multiply fractured isotropic porous media. International Journal of Solids and Structures 43, 3960–3982.

McDermott, C., Kolditz, O., 2006. Geomechanical model for fracture deformation under hydraulic, mechanical and thermal loads. Hydrogeology Journal 14, pp. 485–498.

Pouya A., Ghabezloo S. 2010. Flow around a crack in porous matrix and related problems. Transport in Porous Media, 84, 511–532. Erratum (533).

Rajagopal, K., Tao, L., 1995. Mechanics of mixtures. Series on Advances in Mathematics and Applied Sciences, vol. 35. World Scientific Publishing, Singapore.

Rethore, J., de Borst, R., Abellan, M., 2007. A two-scale approach for fluid flow in fractured porous media. International Journal for Numerical Methods in Engineering 71, 780–800.

Rethore, J., de Borst, R., Abellan, M., 2008. A two-scale model for fluid flow in an unsaturated porous medium with cohesive cracks. Computational Mechanics 42, 227–238.

Sun, D., Gu, W., Guo, X., Lai, W., Mow, V., 1999. A mixed finite element formulation of triphasic mechano-electromechanical theory for charged, hydrated biological soft tissues. International Journal for Numerical Methods in Engineering 45, 1375–1402.

Truesdell, C., 1969. Rational Thermodynamics. McGraw-Hill series in Modern Applied Mathematics.

Vernerey, F., Farsad, M., 2011. An eulerian/xfem formulation for the large deformation of cortical cell membrane. Computer Methods in Biomechanics and Biomedical Engineering 14, 433–445.

Vernerey, F., Liu, W., Moran, B., 2007a. Multi-scale micromorphic theory for hierarchical materials. Journal of the Mechanics and Physics of Solids 55, 2603–2651.

Vernerey, F., Liu, W., Moran, B., Olson, G., 2007b. A micromorphic model for the multiple scale failure of heterogeneous materials. Journal of the Mechanics and Physics of Solids 56, 1320–1347.

Yvonnet, J., Le Quang, H., He, Q., 2008. An xfem/level set approach to modelling surface/interface effects and to computing the size-dependent effective properties of nanocomposites. Computational Mechanics 42, 119–131.

Zhou, C., Sharma, R., Chen, Y., Rong, G., 2008. Flow-stress coupled permeability tensor for fractured rock masses. International Journal for Numerical and Analytical Methods in Geomechanics 32, 1289–1309.